technologies

MDPI

Review

Solid-State Transformers: A Review—Part II: Modularity and Applications

Dragoș-Mihail Predescu [1] and Ștefan-George Roșu [2,*]

[1] Faculty of Electrical Engineering, National University of Science and Technology POLITEHNICA Bucharest, 060042 Bucharest, Romania; dragos.predescu@stud.electro.upb.ro
[2] Faculty of Electronics, Telecommunications and Information Technology, National University of Science and Technology POLITEHNICA Bucharest, 060042 Bucharest, Romania
* Correspondence: stefan.rosu@upb.ro

Abstract: The Solid-State Transformer (SST) is a complex conversion device that intends to replace the Low-Frequency Transformers (LFTs) used in various power applications with Medium- or High-Frequency Transformers (MFTs/HFTs) that integrate modular converter structures as their input and output stages. The purpose is to obtain additional capabilities, such as power factor correction, voltage control, and interconnection of distributed supplies, among others, while reducing the overall volume. Given the expansive research conducted in this area in the past years, the volume of information available is large, so the main contribution of this paper is a new method of classification based on the modular construction of the SST derived from its applications and available constructive degrees of freedom. This paper can be considered the second part of a broader review in which the first part presented the fundamental converter roles and topologies. As a continuation, this paper aims to expand the definition of modularity to the entire SST structure and analyze how the converters can be combined in order to achieve the desired SST functionality. Three areas of interest are chosen: partitioning of power, phase modularity, and port configuration. The partitioning of power analyzes the fundamental switching cells and the arrangement of the converters across stages. Phase modularity details the construction of multiphase-system SSTs. Finally, the types of input/output ports, their placements, and roles are discussed. These characteristics are presented together with the applications in which they were suggested to give a broader context.

Keywords: solid-state transformer; power electronics; isolated converter; multilevel; multicell; modular converter; phase modularity; multiport

check for updates

Academic Editors: Spyridon Nikolaidis, Xiaodong Yang, Juan Wei, Xiaoshun Zhang and Da Xu

Received: 12 December 2024
Revised: 30 December 2024
Accepted: 7 January 2025
Published: 28 January 2025

Citation: Predescu, D.-M.; Roșu, Ș.-G. Solid-State Transformers: A Review—Part II: Modularity and Applications. *Technologies* **2025**, *13*, 50. https://doi.org/10.3390/technologies13020050

Copyright: © 2025 by the authors. Licensee MDPI, Basel, Switzerland. This article is an open access article distributed under the terms and conditions of the Creative Commons Attribution (CC BY) license (https://creativecommons.org/licenses/by/4.0/).

1. Introduction

As the basic functionality of the SST is the generation of an intermediary medium-frequency wave, various implementations have been proposed over the years. This has resulted in vast and diverging implementations and concepts that are part of SST configurations. To allow for an adequate analysis, a two-part review was considered appropriate, with each part's relevant topics represented in Figure 1. The first part classified SSTs based on the number of conversion stages and analyzed converter topologies in that context. This review represents the second part, and it focuses on presenting a new division of information and classification on the modular structure of the SST and contextualizing the structures by pairing them with applications. This is conducted with the purpose of expanding the concept of modularity to the whole SST structure and generalizing the building blocks of the SST. Unless necessary, the stages of conversion are presented with

generic converter blocks, as their specific topology is not of importance, but rather, in this review, the SST as a whole is analyzed. In contrast to the first part, in which the general structure had a secondary role, we define the converter functionalities to allow the selection of fitting topologies. The applications that are presented below are mainly from the areas of energy storage, renewable supplies, distributed systems, and traction. By showcasing the ways in which SSTs can be modified to suit the particularities of such distinct fields, the advantages of modularity can be put into perspective.

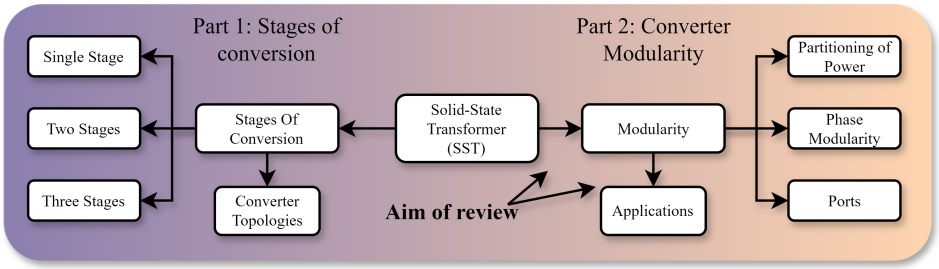


Figure 1. The fundamental Solid-State Transformer structure covered in the two-part review, classified by stages of conversion and modularity

Before analyzing modularity, it is necessary to define it. Traditionally, modularity in the context of power electronics relates to the use of multiple converter modules to expand the power-handling capabilities and maintain functionality during partial module failure. Modularity in the context of this paper represents the usage of a certain degree of freedom available when designing an SST to accommodate the particularities of a given application. As such, an implementation may be modular in some aspects but not others. Solid-State Transformers can be highly modular structures. This is owed to their multi-stage construction, each stage being reduced to just a few simple tasks (folding, current/voltage shaping, isolation, etc.) and various topologies, these concepts having been detailed more broadly in the first part of the review. The following chapters deal with the integration of these topologies into the broader system and the degrees of freedom that are available. Three degrees of freedom are proposed for analysis in this review:

- **Partitioning of power** deals with the fundamental switching cells and the broader arrangement of converter modules. Converters realized with two-level switching cells are limited in both power handling and performance; as such, utilizing switching cells that allow for a higher number of voltage levels is of importance. To further increase the power-handling capabilities, multiple converters may be used at each stage of conversion in various connections, such a structure being called a multicell converter in this review. Modularity in this context means the use of multiple identical switching or converter cells during a stage of conversion to share power and component stresses, whereas non-modular implementations use non-scalable switching cells or use multiple switches in series/parallel.
- **Phase modularity** represents the constructive ways in which an SST is adapted for a multiphase system and how the individual phases are managed during a stage of conversion. SST structures may use a single converter for all phases (non-modular) or separate them into single-phase systems (modular) for various performance and robustness reasons.
- **Ports' configuration** relates to the ways in which the SST structure interacts with external supplies and consumers. The number of ports, their placement, and configuration are analyzed, with multiport implementations representing a modular structure and single input single output, a non-modular one.

Above, modularity was presented in the context of a single stage of conversion; now, it is defined globally. Whereas other reviews have defined it on an axis [1], for simplicity, in this paper it is reduced to one of three classifications: non-modular, fully modular and hybrid modular. Non-modular structures do not have any modular stages, for a particular degree of freedom, with fully modular being the opposite. Hybrid modular represents a middle ground, having at least one modular and non-modular stage. Depending on the placement of the common stage/link or where the ports are connected to, three placements are identified: the HV/MV-DC link, the LVDC link, and the magnetic circuit, which can be referred to as the magnetic link or high-frequency link. While this analysis of modular characteristics mainly focuses on SSTs, it may also be generally applied to similar structures such as the hybrid transformer.

2. Partitioning of Power

Solid-State Transformer applications usually involve the transfer of high power and elevated voltage levels as they aim to replace traditional LFTs. These two facts, combined with the reality that switching devices that can achieve the required switching frequencies have limited voltage/power-handling capabilities, have led researchers to develop many ways to partition the stresses of an SST's switches. As such, this classification details the different ways SSTs have realized this partition of power/voltage on the switching elements. Two alternative concepts are presented. These concepts are not mutually exclusive and have, in fact, been commonly used together in SST applications. They are the use of multilevel switching cells and that of multicell converter arrangements, whose main goal is to increase the number of switching elements and divide the power/voltages across them evenly, lowering the strain on each individual one.

2.1. Fundamental Multilevel Cells

In the previous converter topology paper, the converters were depicted using only diodes and fundamental 2L P/N/P+N switching cells in their construction, with the 2L P+N cell depicted in Figure 2a, with the notable exception of the IAFR-derived rectifiers, but by replacing the fundamental 2L cell with one of the fundamental multilevel cells, depicted in Figure 2b–g, the SST's power-handling capabilities can be significantly improved. By dividing the voltage stress across multiple switching elements while also increasing the number of voltage levels, both breakdown voltages and *dv/dt* stresses are reduced on the switches while also significantly reducing the harmonic content [2–4]. Both voltage and current ripples decrease exponentially with the number of voltage levels [5,6]. The lower *dv/dt* stresses and lower semiconductor area scaling also mean the possibility of higher switching frequencies [7]. These facts, combined with the increase in effective switching frequency, mean that smaller-sized filters can be used [8], which is desired, as one of the characteristics of the SST is its reduced size compared to conventional LFTs. An increase in overall converter efficiency has also been found in multilevel structures compared to two-level ones [3,7]. Additional voltage levels have shown a reduction in current stresses for the isolated converter [9]. These advantages make it a worthwhile tool in the development of high-power SSTs. Such topologies have been successfully implemented in Voltage Source Converters (rectifiers, inverters, indirect AC/AC converters, and matrix converters) [2,10]. The fundamental cells can be broken down into two categories: non-modular and modular. Non-modular cells include the Neutral Point Clamped (NPC), Figure 2b–d, and flying capacitor (FC) family, Figure 2e. In contrast, the modular cells are the Cascaded H-Bridge (CHB), Figure 2f, and the Cascaded Half-Bridge, Figure 2g [2,10]. Theoretically, flying capacitor and NPC topologies can be considered modular, but due to the fact that the number

of capacitors or diodes and the complexity of balancing the voltages across the capacitors increases rapidly with the number of voltage levels, scaling them is not practical [10–13].

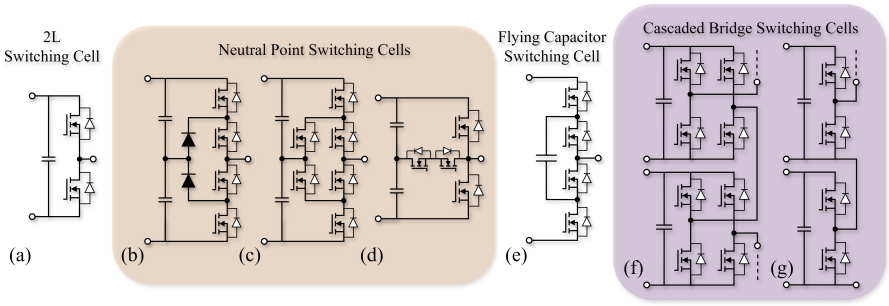


Figure 2. The fundamental (**a**) 2L, (**b**) Neutral-Point-Clamped, (**c**) Active NPC, (**d**) T-type, (**e**) flying capacitor, (**f**) Cascaded Half-Bridge, and (**g**) Cascaded Full-Bridge switching cells.

NPC cells obtain a third output level, zero, by connecting the high- or low-side switches to the midpoint of the DC Link. The ANPC tries to overcome the NPC's unequal loading of the semiconductors and decrease semiconductor losses at the cost of additional switches [10,14]. The T-type cells are NPC cells that connect to the midpoint directly through a bidirectional switch, and rectifiers based on them were presented in the previous paper as the VIENNA, SWISS, and IAF rectifiers. Studies have shown that T-type Cells offer better efficiency compared to NPC cells at medium to high frequencies [15,16]. The NPC family of cells is simple and efficient. Still, due to the low modularity of the structure, cells are usually limited to three levels in applications. However, hybrid cell structures have allowed easy scalability up to five levels [17]. The NPC has been implemented in SST structures both for the rectifier [12,18,19] and the isolated converter [19–23], and a novel implementation of the NPC for the matrix converter can be seen in [24]; T-type topologies are also heavily used in both rectifiers/inverters and isolated rectifiers, as seen in the previous paper, in addition to their use in the isolated converter [9,25]. The three-level ANPC has been suggested for the isolated converter in various configurations [22,26]; similarly, five-level ANPC has been suggested for the rectifier [27] stage and as an isolated AC/AC converter [28] for an SST.

By replacing the diodes of the NPC with capacitors and removing the direct connection to the midpoint, the FC topology can be derived [13]; it is considered more scalable than the NPC family of converters. Other advantages include more switching states, higher redundancy, and the size of the capacitors/voltage imbalance is inversely proportional to the switching frequency [5,11,29]. Compared to NPCs, the FC achieves uniform loading and is more scalable but performs worse at three levels and low frequency [30]. In SST applications, this cell has been suggested for the rectifier and isolated converter [12,31–33], although less prevalently than NPCs.

The Cascaded Half-Bridge and Cascaded H-Bridge topologies, comprised of Half/Full Bridges and a capacitor in series connection, are highly modular, having the least number of capacitors per voltage level, allowing unipolar/bipolar voltages across them, and can achieve the highest efficiency, with the disadvantage of requiring one isolated source for each module, or DC link voltage imbalances [10,29,34]. In SST applications, this structure was used at the input and output stages, in star and delta configurations, connecting the isolated converter to the modules' capacitor [21,32,34–40]. A peculiar application of the CHB is the removal of its capacitor, turning it into a matrix converter [41]. The classical rectifier topologies presented in the previous paper were adapted to higher voltages by replacing the diodes and active switches with Cascaded Half- and Full-Bridges in diverse configurations [42,43].

2.2. Modular Multilevel Converters

Modular Multilevel Converters (MMCs) are multilevel structures in which submodules (SMs), usually Full-Bridge submodules (FBSMs) and Half-Bridge submodules (HBSMs), are placed in series, forming an upper and lower arm, and three ports: positive, negative, and neutral; in the case of a multiphase MMC, they are connected to a common positive and negative terminal, as depicted in Figure 3. Each arm requires its own inductor to limit the second harmonic circulating currents between SMs [44,45]. MMCs have been considered the evolution to the CHBs and Cascaded Half-Bridges [46], which require individual supplies for each module, while the MMC requires only pre-charging of the capacitors; during functioning, the SMs alternate between charging and discharging naturally, which is one of the reasons it has gained popularity in high-power structures, like SSTs [2,44,45,47,48], the other reasons being the higher degree of scalability, redundant cells, reduced volume, simple cell design, multiphase fault tolerance, the addition of the DC port, and cost-effectiveness [48–52].

MMCs can be classified based on the used SMs and their arrangements. The classical SMs are shown in Figure 3d,e, these being the Full- and Half-Bridge Cells. The differences are the generation of a unipolar or, respectively, a bipolar voltage across the SM and better ride-through capabilities for the Full-Bridge SM (FB-SM) at the cost of an increased semiconductor count [51,53] and number of states of the SM; Half-Bridge SMs have two states: charging and discharging. In contrast, FB-SMs have two additional ones: bypass and block. The hybrid MMC, which has more than one type of SM, as seen in Figure 3b, is a structure in which, usually, both the cells shown in Figure 3d,e are used [54], though other novel cells have also been used. Based on the arrangement of these different SMs, the structure can be symmetrical (the arms mirror each other in the arrangement of the SMs) or asymmetrical (each arm contains a unique, different type of SM from the other) [55]. Such a hybrid structure was used to achieve a balance between the fault tolerance of the FB-SM at a reduced component cost [53,54]. Although the SMs are mainly presented as Full and Half Bridges, many other novel configurations, some based upon the fundamental multilevel cells, have been proposed in general applications [44,49,56], as well as directly for SST configurations [57–61]. While most commonly depicted with voltage source SMs, novel current source modules have also been proposed [51], such as in [62], where a current-fed DAB was proposed as an SM, Figure 3f. In SST applications, the SMs have integrated the isolation stage in their construction, the structure being shown in Figure 3c, along with some noteworthy SMs, the current-fed isolated SM (CI-SM) Figure 3f and the matrix-type isolated SM (MI-SM) Figure 3g [59].

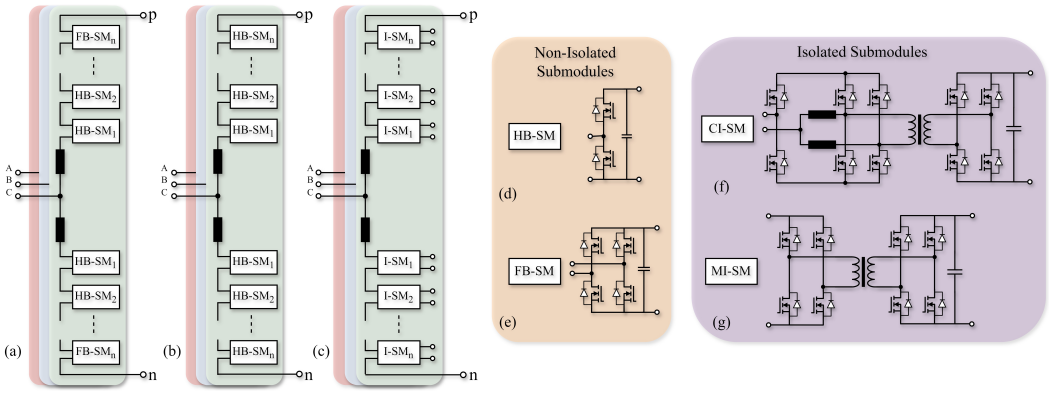


Figure 3. The three-phase (**a**) MMC, (**b**) hybrid MMC, (**c**) isolated SM MMC structures, their non-isolated (**d**) Half-Bridge, (**e**) Full-Bridge, and isolated (**f**) current-fed, and (**g**) matrix submodules (SMs).

The most common implementation of the MMC structure is as a rectifier. During the rectifier stage, MMCs can either act as the legs of an FB rectifier structure, the isolation stages being connected at the DC link [63,64], Figure 4a, or the isolated converters can be cascaded after each SM, as depicted in Figure 4b, creating an additional HV DC link on top of the other intermediary MV and LV DC link and improving SM voltage balancing [45]. Expanding on that idea, in [59], the DABs are configured as the SMs with an added clamp circuit, eliminating the need to balance the capacitor voltages and increasing power density. Other novel implementations have proposed connecting the isolation stage's inputs between two FB SMs, with the output arms acting as the arms of a three-level FC isolated converter [57,58], arguing a reduction in switching elements and short-circuit fault ride through capabilities. In [61], a dual SM configuration was used at the input of the DAB for enhanced fault tolerance. Similarly, a dual clamped cell was proposed in [55], which interleaved two SMs and their DABs. In [65], two MFTs were utilized, one for each polarity of the arms, and they controlled the SMs as the DABs' switches.

In SST applications, this topology has mainly been used for the rectifier stage, Figure 4a,b. However, it has also been proposed for the legs of the isolated converter; a representative configuration is shown in Figure 4c. It must be noted that the MMC has been used for both single/multiphase DAB and FBC/HBC structures in resonant, phase-shifted operating modes [47,50,65–70]. Since each SM needs to switch with a frequency a few times higher than the frequency at the MFT, the overall output frequency at the MFT is restricted, which is not desirable for an SST [47,50,63]. In [62], it was proposed to use DABs, current-fed DABs, and matrix-type DABs as the SMs, thus dealing with the low-switching-frequency problem, while reducing the number of capacitors and achieving bipolar voltages; similarly, in [71]. matrix converters with MF transformers were used as the SMs [59].

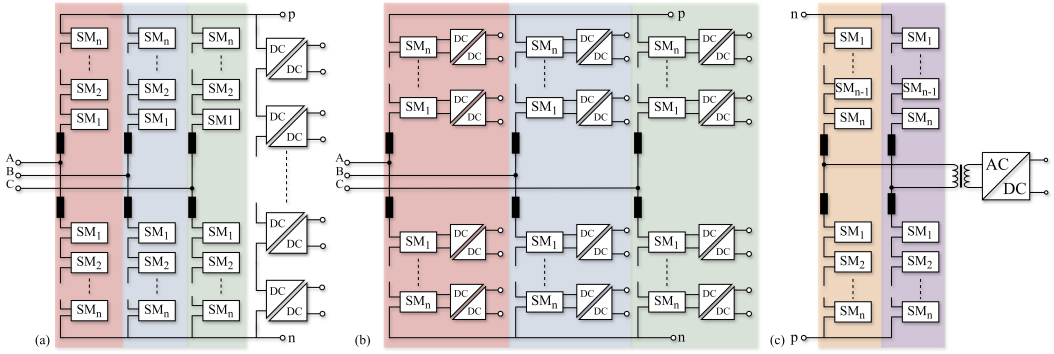


Figure 4. The various applications of the MMC in SST applications: (**a**) rectifier, (**b**) rectifier with cascaded isolation stage, (**c**) isolated converter.

Matrix converters were also proposed for MMC implementations [60,72–74]. A hybrid implementation was proposed in [75], where an MMC indirect matrix DAB was proposed, connected in parallel to an LC filter, creating a DC port. The main applications for the topology are either as the SM cells or as the isolated converter [62,71].

Studies were conducted into the optimal number of SMs per arm in various MMC structures using mathematical models of the topology, its passive components, and multi-objective optimization procedures [76–81]. Across them, maximum voltage across the SM capacitors, circulating currents, minimum reliability, available semiconductors, and the permissible THD of both voltages and currents were seen as design constraints, whereas cost, volume, weight, power losses, SM voltage ripple, and redundancy were usually chosen as optimization goals. By determining the dependency between the optimization goals, the number of cells, the minimum arm inductance, and SM capacitor values, the

optimal number of converter cells can be determined. A general design procedure, utilizing multi-objective optimization is presented in Figure 5.

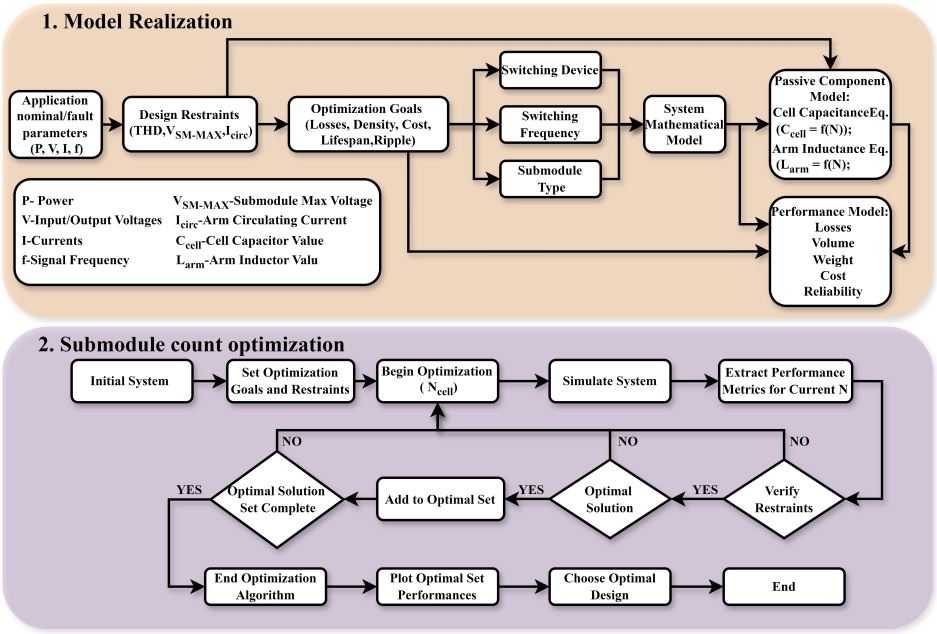


Figure 5. Flowchart of submodule count optimization in two stages, with a step-by-step representation of the mathematical modeling of the system and iterative cell count optimization process.

2.3. Cascaded Multicell Structures

The second method for expanding the power-handling capabilities of SSTs is through the interconnection of the individual converters or cells. As such, instead of distributing the stress on multiple switching elements of a single converter, this method utilizes identical converters that work simultaneously to divide it. Similarly to multilevel cells, the cascading of cell lowers dv/dt, di/dt, and allows for smaller components [50,82]. To determine the optimum number of converter cells, multiple studies have been conducted on multicell converters. The relationship between number of cells and various converter metrics were generalized in [83–85], whereas other studies directly analyzed SST structures and defined mathematical models for the various stages of conversion (AC/DC, DC/DC, isolation stage) [84,86–89] or the effects of converter cell count on MFT performances [90]. Based on said models, and empirical data, the total losses, volume, and reliability of the SST can be determined. Using multi-objective optimization, the optimal configurations can be obtained and their performance plotted to obtain various Pareto fronts, similarly to the process depicted in Figure 5. Overall, the studies show that a balance between conduction and switching losses, the number of active elements and filters, components, and voltage levels must be achieved for a given power/voltage rating as well as an inverse relationship between system redundancy and power density. There is a positive correlation between the number of cells, current ripple, energy density, and converter lifespan. This concept can be considered an extension of MMCs. Compared to other multilevel structures, cascaded cells have a linear cost-voltage level dependency, whereas structures such as ANPCs and FCs have an exponential increase in costs [12].

Depending on the high-current or high-voltage demands, the cells can be interconnected in series or parallel configurations. Parallel connections increase the current-handling capabilities, whereas series ones increase the voltage-handling capabilities. The input and output of the converters may have different connections. Based on these facts, the possible combinations are placed on an input–output stresses axis in Figure 6, from predominantly voltage to predominantly current stresses at both the input and output ports.

As such, they can be classified as input series–output series (ISOP), Figure 6a input parallel–output series (IPOS), Figure 6b, input series–output parallel (ISOP), Figure 6c, or input parallel–output parallel (IPOP), Figure 6d. In high-power applications, such a classification is not sufficient, and converters are placed in both series and parallel connections [91,92]. It is of note that depending on the cell configuration imposed by the application, not all SST structures are viable [93].

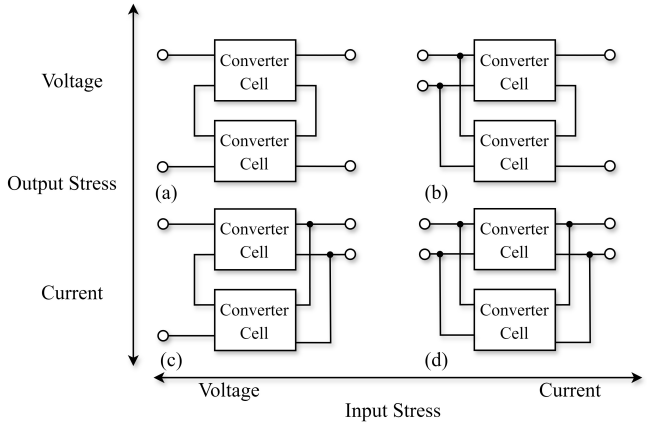


Figure 6. The four converter configurations, (**a**) ISOS, (**b**) IPOS, (**c**) ISOP, (**d**) IPOP, depending on I/O stresses, with series connections handling high voltage and parallel connections high current.

Whereas ISOP and IPOS configurations can achieve voltage balancing between the modules naturally, IPOP and ISOS do not and require additional circuits or careful control [83,94–97]. The cascaded multicell design is inherently redundant, as each stage of the SST may have multiple modules, and each of those modules may be considered independent of each other. As such, if the SST is adequately dimensioned and there is a fault at one or more modules, the remaining ones could compensate for them and maintain, if not nominal, at least partial operation [84,98,99]. In case of a cell failure, if a series connection is used, bypass switches or capacitors are necessary [98,99], although other methods have also been proposed for multicell structures [92,100]. A particular application of this structure is the interleaving of the modules to reduce current ripple, especially in output-parallel configurations, as seen in [101], a similar effect being seen in input-series connections [102]. Converters with output-series configurations have been proposed in multiport applications, where each individual interconnected cell has its individual output port, thus allowing multiple low-voltage consumers to interface with a high-voltage supply [103] or for distributed renewable sources with low voltages to connect to a high-voltage grid [104]. IPOP SST structures have been suggested [46,99], arguing for an improved dynamic response in case of module failure by keeping all modules online even during partial loading.

Novel configurations have also been proposed where the configuration of the cells cannot be reduced to one of the four aforementioned configurations. In [40], an IPOP-S configuration, as depicted in Figure 7a, is proposed for a fast-charger application. The first two stages are in IPOP configuration due to the high current draw of the charger, and then an output series CHM-MC structure is used. An ISOS-P configuration was proposed in [98], where an input series–output series–parallel implementation was used; the design was adapted in Figure 7b. Clusters of converters are connected in the output-series configuration, and the individual clusters are then arranged in interleaved output-parallel configuration. Another such structure is seen in [21] with the difference being that the output-series connection is used to generate a three-voltage level DC port. The input stage has also been proposed for an input-series–parallel connection, particularly when interfacing with renewable supplies. Clusters of solar panels or windmills are placed in series to

step up the voltage and then each cluster is placed in parallel [105]. Further expanding on that concept, a matrix connection was proposed, in which the supplies were placed in series and parallel with each other simultaneously, or the connection was changed through a switch allowing for fast replacement of a faulty module and voltage balancing [92,105,106].

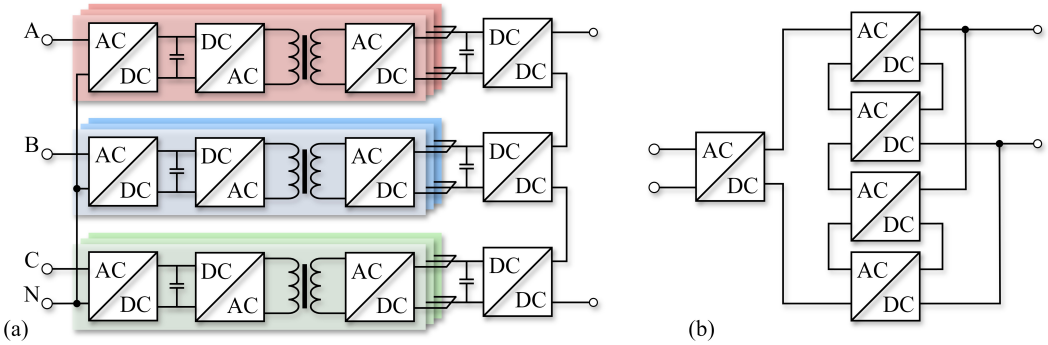


Figure 7. The novel (**a**) input parallel–output parallel–series (IPOP-S) configuration for high-current and variable-output-voltage applications, and (**b**) input series–output series–parallel (ISOS-P) configuration for high-voltage and increased-redundancy applications.

Depending on the application, the converters may connect with each other either after each individual stage, after multiple stages, or only at the input and output of the SST. Because of this, SSTs can be classified by the number of cascaded converter stages, from single converter to hybrid modular and fully modular. Single-cell configurations are limited to low-power/voltage applications or multilevel topologies, whereas fully modular structures utilize multicell arrangements during each stage of conversion and have more freedom in the available topologies/switching cells. Further, below, an analysis of the hybrid configuration, which has some multicell and some single-cell stages, is conducted, analyzing mostly how the rectifier and isolation stages are configured.

If a singular converter cell is used for the rectifier stage, it is usually comprised of either direct-series-connected diodes or an MMC. The isolated converters are either in an input-series configuration at the DC link or placed across the diodes/SMs, such a configuration achieving a lower component count and semiconductor area [50]. In EV charging applications, a popular configuration seems to be a rectifier with a neutral point, followed by two DABs in input-series configuration [107–112] or the use of a DBR with a cascaded boost converter having a neutral point [113]. Input-parallel configurations of the DAB have also been used in charging applications such as [107].

For the isolated converter, if placed in an output-parallel Configuration, the cells have been proposed to connect in one of three places: before the secondary side rectifier [92,114], after it [115], or through the MF magnetic link, such a structure being called a Multi-Active Bridge (MAB), as depicted in Figure 8a, with a brief description of its utilization in multicell applications below and further detailing in Section 4.2. A comparative analysis has shown that multicell implementations of the DAB are more efficient, allow higher switching frequencies, and allow more straightforward control compared to MMC isolated converters [116,117].

The MAB structure, depicted in Figure 8 is similar to the DAB, but instead of two, multiple converter bridges are used this time, which may connect to common or independent ports and/or phases. In this section, it is assumed that only two ports are used, and that the bridges belong to the same phase; in further sections, the uses of the MAB are further expanded. The Multi-Active Bridge uses a common magnetic circuit for the bridges, usually in an asymmetrical configuration, Figure 8a, where one side has multiple active bridges, and the other has only one, thus the cascaded modules converge, and it can be seen as an ISOP structure [21,37,38,118]. There have also been symmetrical configurations in

which both sides have the same number of active bridges [82], Figure 8b, decreasing stress on the LV side but increasing component count; additionally, the MAB has been suggested for use in all four configurations (ISOS, ISOP, IPOP, IPOS) [119]. Another proposed use of the structure is in Dynamic Wireless Power, where multiple transmitter and receiver coils are used to compensate for the variable coupling due to misalignment [120,121]. The advantages of this configuration center around the ability to utilize more DAB modules with a reduced transformer and semiconductor count, thus achieving a higher energy density and reliability [39,82,122]. The main disadvantages of this topology lie in its complexity compared to the classical DAB in both control and transformer design caused by inductive cross coupling between modules, as depicted in Figure 8c. A further analysis on the challenges and proposed solutions can be found in Section 4.2. Although magnetically coupled, in [123], an IPOP Resonant DAB SST is proposed, and consecutive modules are magnetically coupled through the resonant inductors to achieve current balancing. Unlike the MAB, power decoupling between modules is not a problem.

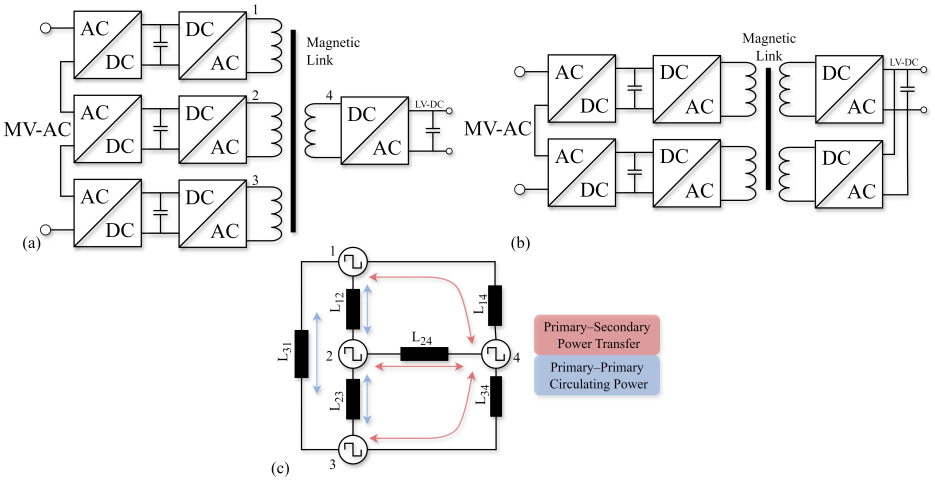


Figure 8. The ISOP (**a**) asymmetrical, (**b**) symmetrical multicell SST Multi-Active Bridge (MAB) structure as well as (**c**) the equivalent model of (**a**) with cross-coupling and resulting circulating power flow between the primary active bridges (1, 2, 3), and the secondary active bridge (4), through the equivalent inductances (L_{12}, L_{23}, L_{31}, L_{34}, L_{14}).

2.4. Overview of Modulation and Control for Converter Structures

Each of the aforementioned switching cells, converter structures, and arrangements has its own particularities. Multiple modulation and control techniques have been proposed to address each one in particular, but such a comprehensive analysis is beyond the scope of this paper. However, a general presentation is in order for multilevel switching cells, MMCs, and multicell structures.

When discussing multilevel switching cells and MMCs, several modulation methods are dominant such as space vector modulation (SVM), pulse-width modulation and its extensions (phase-shifted PWM, sinusoidal pulse-width modulation, selective harmonic elimination PWM, level-shifted, phase disposition, alternate phase opposition disposition, discontinuous PWM), Nearest Level/Vector Control, and Virtual Vector Control [2,13,74,124–126]. Overall control goals for multilevel switching cells revolve around lowering THD and losses, balancing the capacitor voltages, achieving even power/loss sharing, eliminating common-mode voltages, and fault tolerance [2,13,126]. MMCs among the aforementioned goals also aim to reduce circulating currents and SM voltage ripple and eliminate second-order harmonics [12,13,45,73]. Control systems are also varied, including closed-loop PI(D)s, model predictive control [124,127], and Sliding-Mode Control [128,129]. AI integration has also been suggested on multiple occasions regarding control and modula-

tion. Some examples being Particle Swarm Optimization for generating optimal switching states/modulation index [130], the integration of fuzzy logic controllers [131,132], or neural networks [133,134]. Model predictive control has been suggested in applications where multiple parameters are simultaneously controlled, such as neutral-point voltage, power-flow decoupling, converter stability, circulating-current limiting [124,127,135–138]. Multi-stage modulation techniques have also been proposed, although they are still novel [110,139]

1. **Multilevel Switching Cells**
    - **Neutral-Point-Clamped Converters** are limited in some control regards as they cannot achieve even power loss distribution and voltage balancing at more than three levels, using classical modulation, depending on the operating region [10,12,140]. However, they are able to achieve voltage balancing in the classical 3L configuration for all states, and more levels can be achieved if the modulation index is limited [140,141]. Novel modulation techniques have been proposed to attempt to increase the voltage levels for all operating points [125,142], whereas other papers have proposed model predictive control [127]. In [20,26], the modulation of NPC Dual Active Bridges is detailed, presenting the cells' quasi-resonant capabilities, and in [22,143], voltage balancing methods are proposed.
    - **Active Neutral-Point-Clamped Converters** can achieve equal power distribution, and voltage balancing for more than three levels, through the additional switching states introduced by the clamping switches [10,144]. Dual-Active-Bridge modulation has also been extended to the ANPC in [26], where its soft switching conditions are detailed. Other novel implementations have proposed the ANPC to work as a single-stage SST, incorporating modulation principles from totem pole converters and Dual-Active-Bridge phase shifting [28].
    - **Flying capacitor converters** have seen application of PWM multicarrier-based modulation techniques [145]. Control of an isolated DC-DC converter utilizing FC cells is detailed in [31]
    - **Cascaded bridge converters** have increased reliability as they allow redundant states [2]. Control algorithms have been proposed to allow independent capacitor voltage levels for each bridge [146,147]. A slow-start and voltage-balancing procedure for CHBs in SST applications has been realized in [36]. In [43], cascaded bridge topologies are suggested to be incorporated into high-power, active PFC topologies, and their respective modulation/control presented.
2. **Modular Multilevel Converters**, compared to FCs, present superior control capabilities, due to multiple available degrees of freedom, such as energy balancing, loss reduction, arm currents and voltages, etc. [148]. An in-depth review of MMC control objectives, algorithms, as well as a classification of modulation techniques can be found in [60]. Comparative analyses between phase-shifted, and various Phase-Disposition PWM techniques were realized in [44,48,149]. To ensure voltage balancing and even distribution of SM insertion, sorting algorithms based on measured/predicted SM voltages have been proposed [47,48,76]. Hybrid MMCs provide unique challenges compared to single-type SM structures; an analysis of the considerations and adequate control has been conducted in [53,62]. Matrix converters require more advanced control, in contrast to indirect AC/AC topologies, as such MMC integrations of matrix converters, and especially their control, are of note. In [73], a power-decoupling algorithm that manages to realize voltage balancing across arms in matrix MMCs is proposed; in [150], an algorithm to extend fault tolerance is presented, and in [74], Nearest Level Control with an SM voltage-balancing controller is proposed. Given the emergence of novel SMs for SST applications, new commutation steps are proposed, such as in [59] for matrix converter SMs or in [62], where

current-fed DABs are used as submodules in a hybrid MMC and both modulation and control are studied. For MMC isolated converters, resonant modulation/control has been extended in [69,70]. A unique operating mode of the MMC isolated converter is the Quasi-Two-Level (Q2L) modulation [67], which does not have multiple output level voltages, just two, with the transition between these voltage levels controlled by the SM's capacitors, creating a trapezoidal waveform. The capacitors have reduced volume and cost as they are no longer being used for energy storage, but rather for harmonics filtering. This operation allows for higher frequencies at the MFT while maintaining reduced *dv/dt* and capacitor volumes, eliminating common-mode noise and reducing SM volume [67,69,70,151]. The Q2L concept has also been applied to flying capacitor converters [18,152].

3. **Multicell structures** aim to share power equally across modules. Component mismatch and unbalanced supplies/loads may affect this, and as such, the structures require balancing. For ISOP and IPOS arrangements, voltage balancing is natural, whereas IPOP and ISOP configurations require additional considerations [83,94–97].

3. Phase Modularity

The concept of phase modularity refers to the degree to which an SST implementation realizes the independent operation of each phase during the conversion stages, as seen in Figure 9. This usually means using an individual converter and DC Link for each phase. Such an implementation is carried out to increase the redundancy of a system, enhance the current-regulating capabilities to manage unbalanced or distributed supplies/consumers or allow the use of certain topologies that are not available to multiphase systems. Solid-State Transformer implementations have followed this principle to varying degrees and can be grouped into three categories: non-phase-modular, hybrid phase-modular, and fully phase-modular. This section expands upon these categories, define them, and showcase how they have been implemented and their advantages.

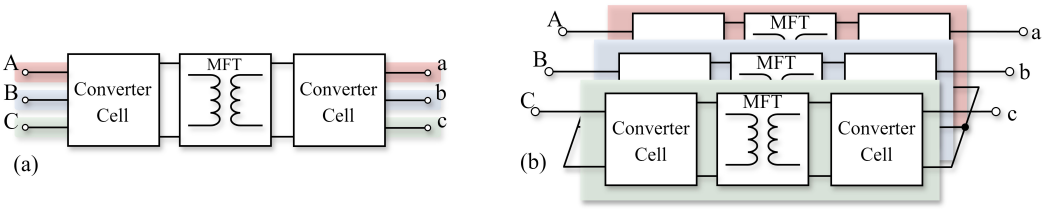


Figure 9. The structure of the (**a**) non-phase-modular and (**b**) fully phase-modular arrangements of the SST.

Non-phase-modular SSTs, depicted in Figure 9a, use a common converter for all stages of conversion, whereas the fully phase-modular SST, represented in Figure 9b can be considered a system comprised of multiple single-phase SSTs, one for each phase, ref. [50] increasing redundancy at the cost of additional components. Regarding control, a clear conclusion cannot be reached as multiphase PFC rectifiers and inverters use more complex modulation techniques than single-phase ones. In contrast, phase-modular configurations require the control of multiple converters and the balancing of their voltages and loadings [19,153,154]. Phase-modular SSTs can either use the line-to-line [155,156] or phase voltage [156,157]. Different analyses have been conducted on the redundancy of phase-modular SSTs, such as in [156], where the control algorithm of the rectifiers changes depending on the state of the phases, normal or faulty, for both wye- and delta-connected SSTs. An interesting approach is the integration of a redundant non-phase-modular SST in IPOP configuration at the inputs/outputs of a phase-modular SST; the redundant module remains online, allowing for a much faster response to phase faults [99].

Fully phase-modular SSTs have been proposed to interface distributed DC supplies to the grid. The supplies are placed in clusters, each cluster connected to one of the grid's phases [104,158]. This configuration also has the advantage of being able to use rectifier topologies only available to single-phase systems such as totem pole and bridgeless boost, as seen in [154,159]. Matrix converters are sensitive to unbalanced input voltages. As such, a phase-modular approach where single-phase matrix converters are used eliminates this deficiency [160–163]. If single-phase SSTs are considered for this classification, their designs could be integrated into a fully phase-modular SST.

A peculiar structure is the hybrid phase-modular one, where only a part of the stages are phase-modular. Compared to the other two categories, which are simple to characterize, this one cannot, as its structure varies depending on the placement of the common stage. The common stage's placement differs from one implementation to another, usually the isolation stage or the LVDC link. Hybrid configurations are analyzed based on where the common-phase configuration begins. It is of note that in single-stage SSTs, due to the lack of a DC link, such a classification may not apply. In [164], a hybrid-phase implementation was proposed, where the MV side converter was phase-independent, but the LV side one was not. However, it could be considered that the isolation stage was where the phases connected to each other in that configuration. Another hybrid-phase implementation that cannot be classified by the aforementioned criteria is seen in [99], where in parallel with a phase-modular SST was placed a common-phase one for redundancy purposes.

During the isolation stage, a common-phase structure is usually achieved using a singular magnetic circuit, as shown in Figure 10a, and proposed/implemented in [165,166]. This configuration, as such, can be considered a MAB and has several advantages, some being the inherent voltage balancing of output-series-connected converters [165,167], improved and centralized power balancing/control capabilities, a reduced magnetic circuit [82,168], and an overall reduction in the transformer RMS current [169]. The balancing of the different phases of the converter cells in such a configuration is achieved by either using a common iron core [165] or by using a secondary voltage-balancing winding on the LV side of the transformer of each phase and then connecting the windings to each other [167]. In [160,166,170], the common magnetic circuit is used for the realization of a 12-pulse rectifier on the LV side to reduce filter size. Due to the common magnetic circuit, the MV inverters can be operated in an open loop. Without sharing the same magnetic circuit, as shown in Figure 10b, this configuration can be realized by placing the LV side of the isolation stage in series before the rectification stage [171,172] or by using a multi-leg inverter on the common-phase side [169] or through a method called synchronous coupling, proposed in [173].

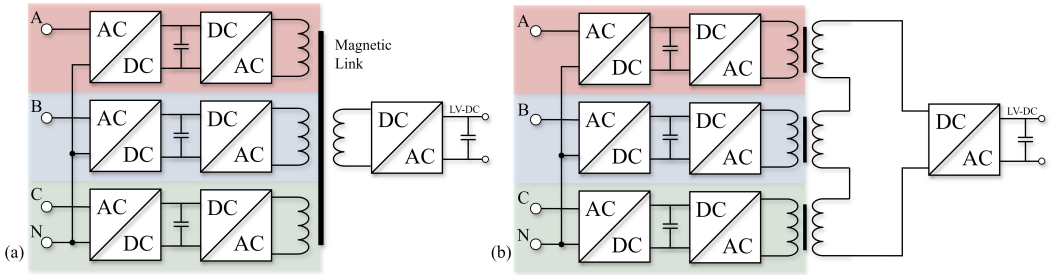


Figure 10. Common-phase isolation stage configuration using (**a**) a common magnetic core and (**b**) series-connected windings.

The most prevalent hybrid phase-modular arrangement seems to be the common LVDC link, whose general depiction is given in Figure 11. This has been usually implemented in AC/DC SSTs for applications where the isolation stages' rectifier DC link is used

as output [112,163,171,172]. In [162], and the interleaving of the isolation stages' outputs is proposed to reduce the current ripple at the common DC link. Another reason for a hybrid configuration is the voltage difference between the MV and LV sides. Lower voltages mean both higher reliability of the converter and the availability of simpler topologies; as such, on the MV and isolation sides, a phase-modular approach is used due to the demands of the application, and on the LV side, a cheaper/simpler option can be used. For example, in [155], to reduce the volume of the capacitors, a phase-modular approach was chosen due to the high voltages. Still, on the LV side, a singular inverter was considered sufficient. In [40], a common output stage was suggested to ensure the equal loading of the phases.

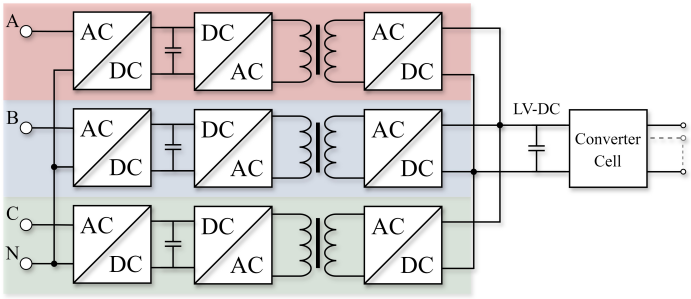


Figure 11. The hybrid phase-modular common LVDC link three-stage SST.

4. Port Modularity

Solid-State Transformer implementations have used the structure's inherent multi-stage and modular capabilities to connect multiple sources and consumers to a singular SST converter. The way in which the SST integrates multiple sources and consumers pertains to its port-modular configuration, various such port configurations being shown in Figure 12. In contrast to prior modularity classifications, SSTs can be non-port-modular or port-modular, but further distinctions can be made when analyzing port-modular implementations. Non-port-modular structures are where a singular input is directly connected to a singular output through the SST. While port-modular configuration can be classified by multiple criteria, the following were chosen for the purpose of this review: type and arrangement. This classification represents the first part of the section; additionally, the construction and control of the MAB are discussed, and a general analysis of multiport SST control is presented.

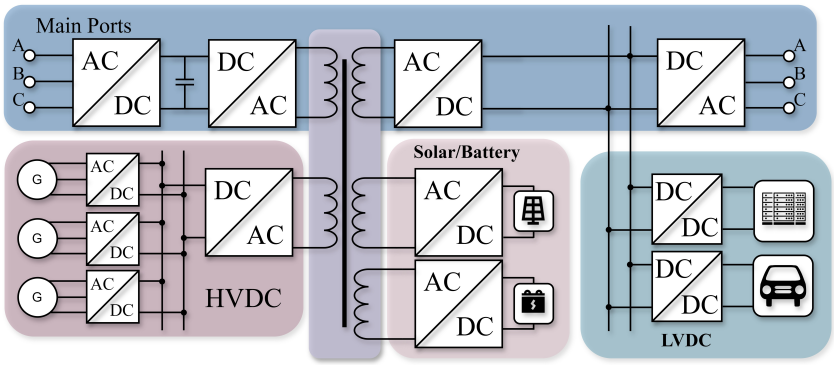


Figure 12. Multiport capabilities of the Solid-State Transformer, depicting a magnetic and LVDC link for interconnection of various consumers, sources, and storage elements.

4.1. Classification of Ports

The type of port can be seen either from a functional point of view as input, output, and bidirectional or from a hierarchical point of view; they can be main or intermediary/auxiliary ports. The main ports are placed at the beginning of the first converter stage

and at the output of the last one, respectively, and represent the main power source/transfer of the SST. In contrast, the intermediary ports are placed between the converter stages and are for lower-importance loads or energy storage purposes. Non-port-modular configurations have only main ports; in a port-modular approach, one or multiple intermediary ports may be present, but it is not necessary to fit the modular criteria. The intermediary port may be an input or output, AC or DC, depending on which stage it is connected to. A novel hybrid input/output port is proposed in [174] where a matrix DAB structure is proposed for EV charging and motor drive applications. During the charging process, the secondary side of the DAB acts as a rectifier and charges the battery; after charging is complete and the primary side is disconnected, the secondary-side converter switches to driving mode, inverting the battery voltage to control the motor. These ports can be placed at the HV/MV/LVDC links or in the magnetic circuit; moving forward, the reason behind such placements is discussed. HV/MVDC link ports connect high-density energy storage systems to HVDC lines [175]. In applications where the HV/MVDC link becomes the output port, the last stages of multiple SST structures may be connected, as seen in [176,177], and it is a desirable configuration in offshore applications to create an HVDC undersea line or in airborne wind turbine applications [178]. During the isolation stage, multiport configurations use topologies such as MABs. They can merge multiple SSTs at the magnetic link, as seen in [39,179]. This configuration was also proposed as a modern UPS alternative [180]. In [175], it was suggested to separate critical and non-critical loads. Another popular application for them is in-phase-modular renewable supply integration, as seen in applications such as [158], where a phase-modular AC/DC SST is used, clusters of solar panels being used to transfer power into each phase of the grid, and to ensure equal current injection into the phases, a battery system is connected to each of the solar panels via MABs. A similar concept was used in [181], with the difference that the solar panels and batteries were connected through intermediary ports and used to balance the voltages of the SST's MMCs, whereas in [165], the magnetic link was used as a voltage bus for the various consumers in a data center, connecting AC and DC supplies/consumers. Similarly, the concept has been extended to grids in [182,183]. Although most commonly used with DABs, resonant configurations have also been proposed in multiport applications [184]. The LVDC ports are usually encountered in hybrid/smart-grid applications to connect LV DERs and DESs [108,162,185], in the DC link consisting of the overhead lines of a railway, maintaining constant voltage from substation to substation and incorporating distributed power supplies [117], or in AC/DC SSTs, for EV charging stations [91,186] or data centers [187].

Port types can be classified based on their arrangement: single port or multiport, series/parallel, AC single/multiphase, and DC. Multiport structures can be organized in series/parallel configurations for similar reasons to series/parallel connections of converters, with the difference being that the power is partitioned to/from other structures instead of modules of the SST. A parallel connection can be seen in [91,108], where at the same DC Link, multiple DC/DC converters are tied, each having its own consumer. Parallel output ports have been proposed for testing the dynamic response of high-power SSTs by way of energy self-circulation [39]. Whereas series connections have been used to divide the voltage to different consumers, as seen in [33] where the LVDC Link voltage is equally divided across multiple data centers, in [45], or in [34,175,188], a midpoint is added to create variable output voltage ports, balance the LVDC link, or act as a buffer. Input-series connections seem to be limited to renewable supplies where they are used to step up the voltages of the clusters for HVDC transport [21,105,158,176,177,189,190]. Inputs may be both in series and parallel; an interesting configuration is the matrix-interconnected input ports, originally presented in the multicell section, in which the series/parallel configuration of

the input ports changes through the use of switches, as proposed in [105,106]. Based on the total number of input and output ports, from a system-wide perspective, the SSTs port arrangement may also be broadly categorized as single/multiple input–single/multiple output (SISO, SIMO, MISO, MIMO).

4.2. Multi-Active Bridges (MAB)

Given the prevalence of the MAB in previous sections, see Sections 2.3, 3 and 4, and the specific characteristics that were presented at each mention, a general characterization of the MAB is in order. The Multi-Active Bridge is an isolated DC/DC converter with multiple cells and a singular, common magnetic core. The MAB may be arranged in symmetrical (equal number of cells on both sides) or asymmetrical (uneven cell distribution) configurations [119], and varying bridge or matrix converter topologies/arrangements may be used [41,119,191]. They can be used to extend power-handling capabilities (Section 2.3), connect multiphase systems (Section 3), and integrate multiple ports (Section 4). The advantages of using the structure were presented alongside the suggested application; however, significant challenges arise. To address them, two areas were chosen for further discussion: control and hardware.

From the control point of view, the inherent coupling of the same side winding makes controlling, balancing, and decoupling power transfer between modules more challenging [37,39,114]. An equivalent model of such an MAB is shown in Figure 8c, depicting the cross-coupling of the bridges. Different control methods have been proposed to account for this, either at the system level [19,37,158,192], or locally for each bridge [39,193–197]. For multicell implementations, balancing the power between MAB modules can be sufficient and was addressed in [19,37], whereas in multiport applications, this is not acceptable [39]. Various decoupling control methods have been proposed, such as feed-forward decoupling [195,196], decoupling matrix [158,192,198,199], multi-loop disturbance rejection [200], time-sharing [184,198], adaptive resonance [201], model predictive control [202], using machine learning/neural networks [203,204], or modified modulation such as multiple/asymmetric phase shift [197] or phase disposition [38].

From a hardware point of view, the multi-winding transformer is more complex than a regular one; the currents in the circuit are higher, leakage inductance becomes a significant design parameter, and scalability is harder (although offset by the decrease in the number of converter cells and their components) [39,119,122,205,206]. If the phase shift between bridges is different, circulating currents will appear as a result of cross-coupling, to ensure that the required phase shift is constant, the leakage inductance must be identical across bridges [207]. Additional studies show that the effect of cross-coupling decreases as the ratio between secondary and primary inductance increases [193,208]. Hardware design methodologies have been proposed to eliminate the problem of cross-coupling. These include the addition of series resonant C/LCs [209–213], non-resonant leakage inductors [193,205,206] or blocking capacitors [214], special magnetic circuit designs that ensure low mutual coupling [215–220], and the use of Diode Bridge or Semiactive Bridge Rectifiers on the secondary side [184,208,221]. Current-fed MABs [222] may also have decoupled power flow.

4.3. Multiport SST Control

The control of the SST consists of multiple control loops that are designed based on the function they must implement. Typically, the main control loops are the fast current loop and the slow voltage loop that are complemented by specifically tailored additional loops to add functionality based on the working mode of the SST at a given point. The multiport SST control contains specific loops in order to make the multiple converters in each port

interact with each other over the main power port or DC link or other type of main structure present [37,175,223]. Given the interfacing of multiple AC systems, SSTs must have grid synchronization capabilities. To synchronize with the grid, the SST must first be able to accurately measure the grid voltage without distortion [224] and then utilize appropriate control algorithms like voltage control mode or power/current control mode [39]. The control algorithms use pulse-width modulation (PWM) methods like the space vector PWM (SVPWM) [178] to generate the required voltage or current at the input or output of the SST. The use of semiconductor devices like SiC MOSFETs and IGBTs in the converters generate a distortion of the output voltage or current due to the dead-time and on-state voltage drops. The closed-loop configuration of the SST compensates for most of the distortions; however, the use of additional low-level control techniques that identify and compensate for the nonlinearity of the converter at the PWM level [225] increases the performance of the SST.

The multiport implementation of the SST requires several additional control loops or control schemes compared to standalone SSTs [39,180,183,188]:

- Power cross-coupling control to damp the power flow oscillations between the MAB converters [193–195].
- A general control framework implemented in the master controller or converter that communicates with all the ports and ensures a soft startup scheme with power balance between cells and ports [19,36,37,39,193].
- Fault monitoring and mitigation control for situations like DC port short-circuit fault or large transient events [37,119,226].
- Transition control for changing of operation modes like a change in main power port or a change in control from grid forming (voltage control mode) to grid following (power/current control mode) [37,57,210].
- Ensuring the whole system stability for varying loads and transients [227–232].

5. Overview of Modularity

In the past three sections, the modularity of the SST was examined from different perspectives, from a converter construction point of view (the various switching cells), the arrangement of the converters, the connection of the phases, and the placement of the ports. Figure 13 showcases a summary of the various constructive elements of the SST, integrating essential elements from both the first and second part of the review. To highlight the difference between modular and non-modular implementations for each of the three degrees of freedom, based on the information presented in this paper, the elements were color-coded. Green means that the element/configuration/structure is modular whereas red is non-modular, orange was used to signify areas that could be either depending on implementation or to represent a hybrid modular approach. Blocks that were not colored were considered to not impact the modularity of the structure. For example, the arrangement of the ports could be used to allow a modular implementation of the port configuration's degree of freedom, depending on whether a single port (non-modular) or multiport (modular) arrangement was chosen. Flying-capacitor switching cells were color-coded orange because their modularity/scalability is debatable. The number of stages is irrelevant as structures used in all three variations could be modular or not.

Starting with the SST block, two different partitions of characteristics are presented:

- The partition in Figure 13 focuses on the available elements during the realization of the SST. Four areas of interest were identified across the two-part review: **stages (of conversion) (in Part I)**, **port (configurations)**, **phase (modularity)** and **converter (structures)**.

1. **Stages (of conversion)**, ranging from one to three, determine the functionalities that the converters must cover and the available topologies, with a detailed analysis presented in Part I.
2. **Port (configurations)** cover the arrangement of the ports, covering single-port (non-modular) and multiport (modular) implementations; their hierarchy: main ports (modularity depends on implementation) or intermediary ports (modular); as well as their purpose: input/output in case of unidirectional systems or dual purpose for bidirectional ones.
3. **Phase (modularity)** relates to the partition of phases across converters and the transformer, and the choice whether to separate them or not (modular vs. non-modular approach).
4. **Converter (structures)** have been presented using two characteristics: the switching cells and the arrangement of modules. Switching cells can be non-modular (2L, NPC), or modular (cascaded Half/Full Bridges), the distinction between the two categories being the scalability of the switching cell to multiple voltage levels. Modular Multilevel Converters are an extension of the concept. The arrangement of the converters covers the use of one (non-modular) or multiple (modular) converters. In the case of multiple converter cells, they can be arranged in different configurations at their inputs and outputs.

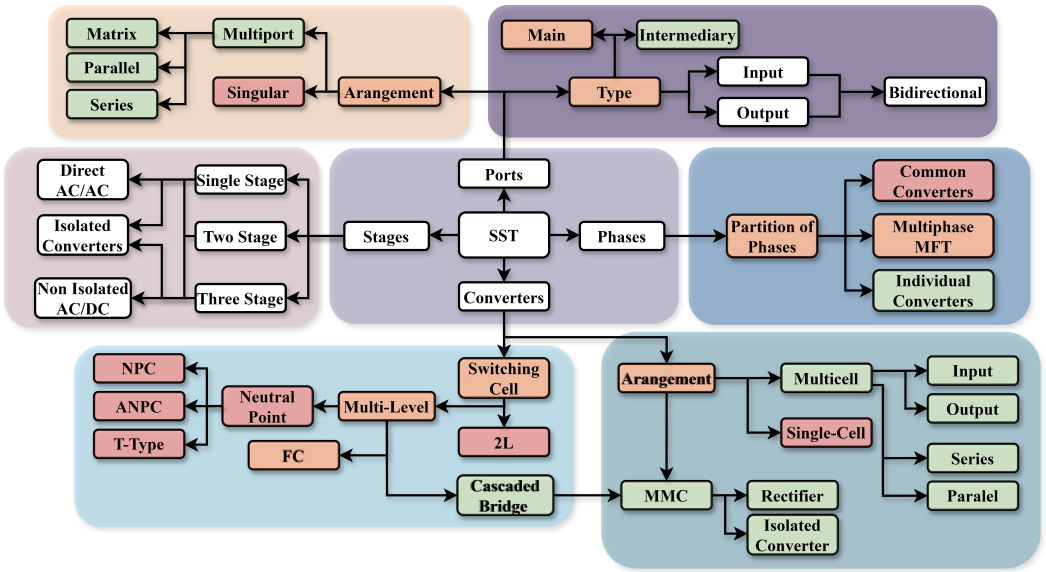


Figure 13. Overview of the Solid-State Transformer structure and classification parameters: stages, ports, phases, and converters and a color classification of their modular characteristics (red—non-modular, orange—hybrid modular, green—modular).

- The partition in Figure 14 focuses on a top-down analysis of the relationship between design stages. In this context the SST can be defined by the context of its **application**, the **control** methods and the three proposed **degrees of freedom**.
    1. **The application** dictates the requirements of the structure, and based upon its particularities, different design choices can be made utilizing the available **degrees of freedom** to optimize performance.
    2. **Control** of the SST represents the control algorithms and modulation techniques used at both the system level and across the individual converters. Available control methods impact the **degrees of freedom**, but also based on the chosen implementation, the control system must be adapted.

3. **Degrees of freedom** represent the ways in which a system can be adapted to suit a given application. The three identified degrees were analyzed at large throughout the review, and the use of such degrees has been quantified through the term modularity and was given one of three ratings: non-modular (no modular stages), hybrid modular (some modular stages), and fully modular (all stages are modular). The ratings are independent for each degree of freedom. Hybrid modular implementations were further classified by the common stage.

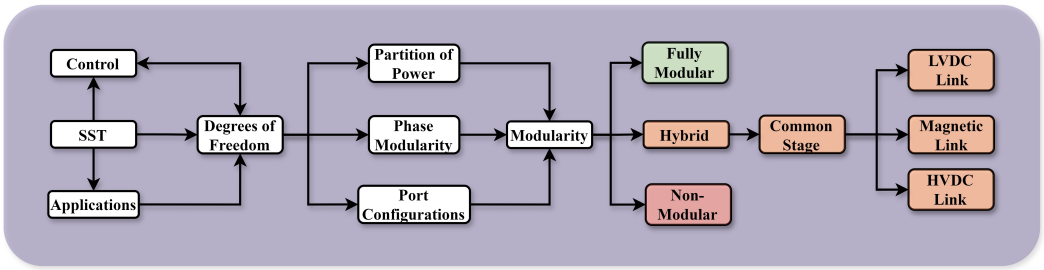


Figure 14. Overview of the Solid-State Transformer design stages: applications, control algorithms and constructive degrees of freedom, as well as the relationship between them.

Areas of Future Research

Regarding the modular structure of the SST, several interesting directions of research are presented:

1. Whereas the fundamental, voltage-source multilevel switching cells have been incorporated into the SST's converters, hybrid and current-fed cells have not been implemented.
2. Papers suggesting incorporating the MMC structure into other rectifier topologies, such as the VIENNA rectifier, have promising results but physical implementation is needed to validate them.
3. Incorporating the isolation stage into the submodules has been suggested as an effective way to reduce costs and volume in high-power applications.
4. Q2L modulation seems fitting for high-power single- and two-stage SSTs, particularly for the isolated converter, as it does not limit the frequency of the signal passing through the MFT.
5. Regarding cascaded multicell structures, hybrid arrangements of SMs could see further research.
6. In phase-modular systems, novel ways have been proposed to increase redundancy and balance the phases; these directions of research are of note.
7. Novel port configurations such as series-connected outputs and matrix inputs show the most potential for further study as they allow scalability and redundancy.
8. Among all three categories of modularity, the Multi-Active Bridge configuration has been proposed, and its many benefits have been presented from multiple perspectives, but the difficulty of decoupling power flow across the bridges combined with the difficult transformer design hold it back and require further analysis to streamline its design.

6. Conclusions

The presented review showcased past and current trends of SST structures, with an emphasis on their construction at the system level. To do such an analysis, three categories were defined: converter structure modularity, phase modularity, and port modularity. These categories allowed us to analyze the modularity of the structure, establishing how the converters were interconnected to increase different capabilities of the SST, such as power rating, voltage control, interfacing of multiple consumers, increase in redundancy, power

density, and efficiency. For converter structures, different switching cells and arrangements of converters were analyzed. In contrast, phase modularity discussed how the different phases of the SST interacted with each other, and port modularity showcased the different ways in which the SST interacted with external structures, be they consumers or sources. Each modular characteristic was further divided into non-modular, fully modular and hybrid modular. When dealing with hybrid modular structures, the energy storage links were considered points of interconnection. These links were the medium/high-voltage DC link, the low-voltage DC link and the magnetic link or high-frequency link. As the amount of research on SSTs is comprehensive, a two-part review was considered necessary, this being the second part.

Author Contributions: Methodology, D.-M.P. and Ș.-G.R.; writing—original draft preparation, D.-M.P.; writing—review and editing, D.-M.P. and Ș.-G.R.; supervision, Ș.-G.R.; funding acquisition, Ș.-G.R. All authors have read and agreed to the published version of the manuscript.

Funding: This research was funded by a grant from the National Program for Research of the National Association of Technical Universities—GNAC ARUT 2023, project ID198-nr.162-04.12.2023.

Institutional Review Board Statement: Not applicable.

Informed Consent Statement: Not applicable.

Data Availability Statement: Data sharing is not applicable.

Conflicts of Interest: The authors declare no conflicts of interest.

References

1. Shamshuddin, M.A.; Rojas, F.; Cardenas, R.; Pereda, J.; Diaz, M.; Kennel, R. Solid State Transformers: Concepts, Classification, and Control. *Energies* **2020**, *13*, 2319. [CrossRef]
2. Rodriguez, J.; Franquelo, L.; Kouro, S.; Leon, J.; Portillo, R.; Prats, M.; Perez, M. Multilevel Converters: An Enabling Technology for High-Power Applications. *Proc. IEEE* **2009**, *97*, 1786–1817. [CrossRef]
3. Azurza Anderson, J.; Zulauf, G.; Papamanolis, P.; Hobi, S.; Miric, S.; Kolar, J.W. Three Levels Are Not Enough: Scaling Laws for Multilevel Converters in AC/DC Applications. *IEEE Trans. Power Electron.* **2021**, *36*, 3967–3986. [CrossRef]
4. Qashqai, P.; Sheikholeslami, A.; Vahedi, H.; Al-Haddad, K. A Review on Multilevel Converter Topologies for Electric Transportation Applications. In Proceedings of the 2015 IEEE Vehicle Power and Propulsion Conference (VPPC), Montreal, QC, Canada, 19–22 October 2015; pp. 1–6. [CrossRef]
5. Lei, Y.; Barth, C.; Qin, S.; Liu, W.C.; Moon, I.; Stillwell, A.; Chou, D.; Foulkes, T.; Ye, Z.; Liao, Z.; et al. A 2-kW Single-Phase Seven-Level Flying Capacitor Multilevel Inverter with an Active Energy Buffer. *IEEE Trans. Power Electron.* **2017**, *32*, 8570–8581. [CrossRef]
6. Meynard, T.; Foch, H.; Thomas, P.; Courault, J.; Jakob, R.; Nahrstaedt, M. Multicell converters: Basic concepts and industry applications. *IEEE Trans. Ind. Electron.* **2002**, *49*, 955–964. [CrossRef]
7. Schweizer, M.; Lizama, I.; Friedli, T.; Kolar, J.W. Comparison of the chip area usage of 2-level and 3-level voltage source converter topologies. In Proceedings of the IECON 2010—36th Annual Conference on IEEE Industrial Electronics Society, Glendale, AZ, USA, 7–10 November 2010; pp. 391–396. [CrossRef]
8. Lei, Y.; Liu, W.C.; Pilawa-Podgurski, R.C.N. An analytical method to evaluate flying capacitor multilevel converters and hybrid switched-capacitor converters for large voltage conversion ratios. In Proceedings of the 2015 IEEE 16th Workshop on Control and Modeling for Power Electronics (COMPEL), Vancouver, BC, Canada, 12–15 July 2015; pp. 1–7. [CrossRef]
9. Yadeo, D.; Chaturvedi, P.; Lai, J.S.J.; Suryawanshi, H.; Saketi, S.K. A T-type dual active bridge with symmetrical configuration for solid state transformer. *Int. J. Electron.* **2021**, *108*, 2019–2038. [CrossRef]
10. Kouro, S.; Malinowski, M.; Gopakumar, K.; Pou, J.; Franquelo, L.G.; Bin, W.; Rodriguez, J.; Pérez, M.A.; Leon, J.I. Recent Advances and Industrial Applications of Multilevel Converters. *IEEE Trans. Ind. Electron.* **2010**, *57*, 2553–2580. [CrossRef]
11. Rao, A.P.C.; Obulesh, Y.P.; Babu, C.S. Analysis and effect of switching frequency and voltage levels on total harmonic distortion in multilevel inverters. In Proceedings of the 2012 International Conference on Emerging Trends in Electrical Engineering and Energy Management (ICETEEEM), Chennai, Tamil Nadu, India, 13–15 December 2012; pp. 339–344. [CrossRef]
12. Van Der Merwe, W.; Mouton, T. Solid-state transformer topology selection. In Proceedings of the 2009 IEEE International Conference on Industrial Technology, Churchill, VIC, Australia, 10–13 February 2009; pp. 1–6. [CrossRef]

13. Hasan, N.S.; Rosmin, N.; Osman, D.A.A.; Musta'amal@Jamal, A.H. Reviews on multilevel converter and modulation techniques. *Renew. Sustain. Energy Rev.* **2017**, *80*, 163–174. [CrossRef]
14. Dodge, J. *3L-ANPC vs. 3L-NPC Inverters*; Application Note AN0023; UnitedSiC: Princeton, NJ, USA, 2021.
15. Stecca, M.; Soeiro, T.B.; Elizondo, L.R.; Bauer, P.; Palensky, P. Comparison of Two and Three-Level DC-AC Converters for a 100 kW Battery Energy Storage System. In Proceedings of the 2020 IEEE 29th International Symposium on Industrial Electronics (ISIE), Delft, The Netherlands, 17–19 June 2020; pp. 677–682. [CrossRef]
16. Lee, K.; Shin, H.; Choi, J. Comparative analysis of power losses for 3-Level NPC and T-type inverter modules. In Proceedings of the 2015 IEEE International Telecommunications Energy Conference (INTELEC), Osaka, Japan, 18–22 October 2015; pp. 1–6. [CrossRef]
17. Kieferndorf, F.; Basler, M.; Serpa, L.; Fabian, J.H.; Coccia, A.; Scheuer, G. *The Five-Level Converter*; Review; ABB: Zürich, Switzerland, 2011.
18. Lu, C.; Hu, W.; Wu, H.; Lee, F. Quasi-Two-Level Bridgeless PFC Rectifier for Cascaded Unidirectional Solid State Transformer. *IEEE Trans. Power Electron.* **2021**, *36*, 12033–12044. [CrossRef]
19. Jeong, D.K.; Yun, H.J.; Park, S.H.; Kim, M.H.; Ryu, M.H.; Baek, J.W.; Kim, H.S. 13.2 kV Class 3-Phase Solid State Transformer System Based on EtherCAT Communication. *Electronics* **2022**, *11*, 3092. [CrossRef]
20. Zhao, X.; Li, B.; Fu, Q.; Mao, S.; Xu, D.; Leon, J.I.; Franquelo, L.G. DC Solid State Transformer Based on Three-Level Power Module for Interconnecting MV and LV DC Distribution Systems. *IEEE Trans. Power Electron.* **2021**, *36*, 1563–1577. [CrossRef]
21. Yun, H.J.; Jeong, D.K.; Kim, H.S.; Kim, M.; Baek, J.W.; Kim, J.Y.; Kim, H.J. Implementation of a Single-Phase SST for the Interface between a 13.2 kV MVAC Network and a 750 V Bipolar DC Distribution. *Electronics* **2018**, *7*, 62. [CrossRef]
22. Filba-Martinez, A.; Busquets-Monge, S.; Nicolas-Apruzzese, J.; Bordonau, J. Operating Principle and Performance Optimization of a Three-Level NPC Dual-Active-Bridge DC–DC Converter. *IEEE Trans. Ind. Electron.* **2016**, *63*, 678–690. [CrossRef]
23. Chen, K.T.; Chen, J.F.; Wang, T.J.; Liao, H. Study and Implementation of High Frequency Cast Resin Transformer Applied for Medium-Voltage Solid-State Transformer. In Proceedings of the 2021 IEEE International Future Energy Electronics Conference (IFEEC), Taipei, Taiwan, 16–19 November 2021; pp. 1–6. [CrossRef]
24. Klumpner, C.; Lee, M.; Wheeler, P. A New Three-Level Sparse Indirect Matrix Converter. In Proceedings of the IECON 2006—32nd Annual Conference on IEEE Industrial Electronics, Paris, France, 6–10 November 2006; pp. 1902–1907, ISSN 1553-572X. [CrossRef]
25. Pham N., H.; Mannen, T.; Wada, K. A Three-Phase Isolated Rectifier using Current Unfolding and Active Damping Methods. In Proceedings of the 2020 IEEE Energy Conversion Congress and Exposition (ECCE), Detroit, MI, USA, 11–15 October 2020; pp. 4587–4593. [CrossRef]
26. Guan, Q.X.; Zhang, Y.; Zhao, H.B.; Kang, Y. Optimized Switching Strategy for ANPC–DAB Converter Through Multiple Zero States. *IEEE Trans. Power Electron.* **2022**, *37*, 2885–2898. [CrossRef]
27. Sotoodehkia, M.; Arasteh, M.; Soleymani Mucheh Khorti, S.; Hoseinpour, M. Design and control strategy of solid state transformer using CHB MMC and 5-L ANPC multilevel converters. *Int. J. Nonlinear Anal. Appl.* **2022**, *14*, 161–179. [CrossRef]
28. Rajendran, S.; Huang, A.Q. A novel Three-level Three-phase Single Stage Solid State Transformer with An Integrated DC Link. In Proceedings of the 2022 IEEE Energy Conversion Congress and Exposition (ECCE), Detroit, MI, USA, 9–13 October 2022; pp. 1–7. [CrossRef]
29. Krug, D.; Bernet, S.; Fazel, S.S.; Jalili, K.; Malinowski, M. Comparison of 2.3-kV Medium-Voltage Multilevel Converters for Industrial Medium-Voltage Drives. *IEEE Trans. Ind. Electron.* **2007**, *54*, 2979–2992. [CrossRef]
30. Fazel, S.S.; Bernet, S.; Krug, D.; Jalili, K. Design and Comparison of 4-kV Neutral-Point-Clamped, Flying-Capacitor, and Series-Connected H-Bridge Multilevel Converters. *IEEE Trans. Ind. Appl.* **2007**, *43*, 1032–1040. [CrossRef]
31. Ghias, A.M.; Ciobotaru, M.; Agelidis, V.G.; Pou, J. Solid state transformer based on the flying capacitor multilevel converter for intelligent power management. In Proceedings of the IEEE Power and Energy Society Conference and Exposition in Africa: Intelligent Grid Integration of Renewable Energy Resources (PowerAfrica), Johannesburg, South Africa, 9–13 July 2012; pp. 1–7. [CrossRef]
32. Borges, V.L.F.; Da Silva, R.L.; Possamai, C.E.; Bettiol, A.L.; Barbi, I. A ISOP AC-AC Hybrid Switched-Capacitor SRC for Solid State Transformer Applications. In Proceedings of the 2019 IEEE 15th Brazilian Power Electronics Conference and 5th IEEE Southern Power Electronics Conference (COBEP/SPEC), Santos, Brazil, 1–4 December 2019; pp. 1–6. [CrossRef]
33. Huber, J.; Wallmeier, P.; Pieper, R.; Schafmeister, F.; Kolar, J.W. Comparative Evaluation of MVAC-LVDC SST and Hybrid Transformer Concepts for Future Datacenters. In Proceedings of the 2022 International Power Electronics Conference (IPEC-Himeji 2022—ECCE Asia), Himeji, Japan, 15–19 May 2022; pp. 2027–2034. [CrossRef]
34. Zhao, T.; Wang, G.; Bhattacharya, S.; Huang, A.Q. Voltage and Power Balance Control for a Cascaded H-Bridge Converter-Based Solid-State Transformer. *IEEE Trans. Power Electron.* **2013**, *28*, 1523–1532. [CrossRef]
35. Elsanabary, A.I.; Konstantinou, G.; Mekhilef, S.; Townsend, C.D.; Seyedmahmoudian, M.; Stojcevski, A. Medium Voltage Large-Scale Grid-Connected Photovoltaic Systems Using Cascaded H-Bridge and Modular Multilevel Converters: A Review. *IEEE Access* **2020**, *8*, 223686–223699. [CrossRef]

36. Pugliese, S.; Buticchi, G.; Mastromauro, R.A.; Andresen, M.; Liserre, M.; Stasi, S. Soft-Start Procedure for a Three-Stage Smart Transformer Based on Dual-Active Bridge and Cascaded H-Bridge Converters. *IEEE Trans. Power Electron.* **2020**, *35*, 11039–11052. [CrossRef]
37. Rahman, M.A.; Islam, M.R.; Muttaqi, K.M.; Sutanto, D. Data Driven Coordinated Control of Converters in a Smart Solid State Transformer for Reliable and Automated Distribution Grids. *IEEE Trans. Ind. Appl.* **2020**, *56*, 4532–4542. [CrossRef]
38. Rahman, M.A.; Islam, M.R.; Muttaqi, K.M.; Guo, Y.; Zhu, J.; Sutanto, D.; Lei, G. A Modified Carrier-Based Advanced Modulation Technique for Improved Switching Performance of Magnetic-Linked Medium-Voltage Converters. *IEEE Trans. Ind. Appl.* **2019**, *55*, 2088–2098. [CrossRef]
39. Wen, W.; Li, K.; Zhao, Z.; Yuan, L.; Mo, X.; Cai, W. Analysis and Control of a Four-Port Megawatt-Level High-Frequency-Bus-Based Power Electronic Transformer. *IEEE Trans. Power Electron.* **2021**, *36*, 13080–13095. [CrossRef]
40. Elserougi, A.; Abdelsalam, I.; Massoud, A. An isolated-boost-converter-based unidirectional three-phase off-board fast charger for electric vehicles. *IET Electr. Syst. Transp.* **2022**, *12*, 79–88. [CrossRef]
41. Iyer, K.V.; Baranwal, R.; Mohan, N. A High-Frequency AC-Link Single-Stage Asymmetrical Multilevel Converter for Grid Integration of Renewable Energy Systems. *IEEE Trans. Power Electron.* **2017**, *32*, 5087–5108. [CrossRef]
42. Makoschitz, M. Unidirectional medium voltage rectifier utilizing sinusoidal input currents. *Electron. Lett.* **2022**, *58*, 474–476. [CrossRef]
43. Jonas, H. *A New Family of Three-Phase-Unfolder-Based MVAC-LVDC Solid-State Transformers*; VDE VERLAG GMBH: Berlin, Germany, 2024. [CrossRef]
44. Barros, L.A.M.; Martins, A.P.; Pinto, J.G. A Comprehensive Review on Modular Multilevel Converters, Submodule Topologies, and Modulation Techniques. *Energies* **2022**, *15*, 1078. [CrossRef]
45. Sun, X.; Teng, J.; Bu, Z.; Pan, Y.; Zhao, W.; Li, X. Research on Triple-Port SST Scheme Based on the Natural Elimination of MMC Submodule Voltage Fluctuation and Imbalance. *IEEE J. Emerg. Sel. Top. Power Electron.* **2022**, *10*, 3697–3710. [CrossRef]
46. Liserre, M.; Buticchi, G.; Andresen, M.; De Carne, G.; Costa, L.F.; Zou, Z.X. The Smart Transformer: Impact on the Electric Grid and Technology Challenges. *IEEE Ind. Electron. Mag.* **2016**, *10*, 46–58. [CrossRef]
47. Kenzelmann, S.; Rufer, A.; Dujic, D.; Canales, F.; De novaes, Y.R. Isolated DC/DC Structure Based on Modular Multilevel Converter. *IEEE Trans. Power Electron.* **2015**, *30*, 89–98. [CrossRef]
48. Debnath, S.; Qin, J.; Bahrani, B.; Saeedifard, M.; Barbosa, P. Operation, Control, and Applications of the Modular Multilevel Converter: A Review. *IEEE Trans. Power Electron.* **2015**, *30*, 37–53. [CrossRef]
49. Raju, M.N.; Sreedevi, J.; P Mandi, R.; Meera, K. Modular multilevel converters technology: A comprehensive study on its topologies, modelling, control and applications. *IET Power Electron.* **2019**, *12*, 149–169. [CrossRef]
50. Rothmund, D.; Ortiz, G.; Kolar, J.W. SiC-based unidirectional solid-state transformer concepts for directly interfacing 400 V DC to Medium-Voltage AC distribution systems. In Proceedings of the 2014 IEEE 36th International Telecommunications Energy Conference (INTELEC), Vancouver, BC, Canada, 28 September–2 October 2014; pp. 1–9. [CrossRef]
51. Nami, A.; Liang, J.; Dijkhuizen, F.; Demetriades, G.D. Modular Multilevel Converters for HVDC Applications: Review on Converter Cells and Functionalities. *IEEE Trans. Power Electron.* **2015**, *30*, 18–36. [CrossRef]
52. Xiong, J.; Li, Y.; Cao, Y.; Panasetsky, D.; Sidorov, D. Modeling and operating characteristic analysis of MMC-SST based shipboard power system. In Proceedings of the 2016 IEEE PES Asia-Pacific Power and Energy Engineering Conference (APPEEC), Xi'an, China, 25–28 October 2016; pp. 28–32. [CrossRef]
53. Zeng, R.; Xu, L.; Yao, L.; Williams, B.W. Design and Operation of a Hybrid Modular Multilevel Converter. *IEEE Trans. Power Electron.* **2015**, *30*, 1137–1146. [CrossRef]
54. Chen, Y.; Ren, C.; Sheng, J.; Wang, J.; Zhou, Y.; Cao, W.; Ding, R.; Wang, W. An Optimized Fault-Ride-Through Control Strategy of Hybrid MMC with Fewer FBSMs. *Electronics* **2024**, *13*, 1797. [CrossRef]
55. Zapico, A.; Lopez, M.; Rodriguez, A.; Briz, F. Fault tolerant cell design for MMC-based multiport power converters. In Proceedings of the 2016 IEEE Energy Conversion Congress and Exposition (ECCE), Milwaukee, WI, USA, 18–22 September 2016; pp. 1–8. [CrossRef]
56. Li, X.; Liu, W.; Song, Q.; Rao, H.; Xu, S. An enhanced MMC topology with DC fault ride-through capability. In Proceedings of the IECON 2013—39th Annual Conference of the IEEE Industrial Electronics Society, Vienna, Austria, 10–13 November 2013; pp. 6182–6188. [CrossRef]
57. Jianqiao, Z.; Jianwen, Z.; Xu, C.; Jiacheng, W.; Jiajie, Z. Family of Modular Multilevel Converter (MMC) Based Solid State Transformer (SST) Topologies for Hybrid AC/DC Distribution Grid Applications. In Proceedings of the 2018 IEEE International Power Electronics and Application Conference and Exposition (PEAC), Shenzhen, China, 4–7 November 2018; pp. 1–5. [CrossRef]
58. Yan, Y.; Sun, Y.; Guo, W.; Jiang, H.; Hu, M. Arm integrated double capacitor submodule for modular multilevel solid-state transformers with DC short-circuit fault ride-through capability. *J. Power Electron.* **2024**, *24*, 862–874. [CrossRef]
59. Liu, C.; Liu, C.; Cai, G.; Ying, H.; Zhang, Z.; Shan, R.; Pei, Z.; Song, X. An Isolated Modular Multilevel Converter (I-M^2 C) Topology Based on High-Frequency Link (HFL) Concept. *IEEE Trans. Power Electron.* **2020**, *35*, 1576–1588. [CrossRef]

60. Bashir, S.B.; Ismail, A.A.A.; Elnady, A.; Farag, M.M.; Hamid, A.K.; Bansal, R.C.; Abo-Khalil, A.G. Modular Multilevel Converter-Based Microgrid: A Critical Review. *IEEE Access* **2023**, *11*, 65569–65589. [CrossRef]
61. Li, D.; Ji, Z.; Sun, Y.; Zhao, J.; Zhang, C. Four-port solid-state transformer based on hybrid MMC with enhanced dual half-bridge submodules. *IET Power Electron.* **2020**, *13*, 2432–2441. [CrossRef]
62. Pei, Z.; Kong, D.; Liu, C.; Liu, C.; Guo, D.; Zhu, D.; Sun, Y.; Heldwein, M.L. Hybrid Isolated Modular Multilevel Converter Based Solid-State Transformer Topology with Simplified Power Conversion Process and Uneven Voltage Ratio. *IEEE Trans. Power Electron.* **2023**, *38*, 12757–12773. [CrossRef]
63. Adabi, M.E.; Martinez-Velasco, J.A.; Alepuz, S. Modeling and simulation of a MMC-based solid-state transformer. *Electr. Eng.* **2018**, *100*, 375–387. [CrossRef]
64. Linlin, B.; Danni, C.; Jianlong, Z.; Wanyu, J. Topology and Control Strategy Improvement of Middle Stage of Power Electronic Transformer Based on Modular Multilevel Converter. In Proceedings of the 2019 4th International Conference on Power and Renewable Energy (ICPRE), Chengdu, China, 21–23 September 2019; pp. 259–263. [CrossRef]
65. Ma, D.; Chen, W.; Shu, L.; Qu, X.; Hou, K. A MMC-Based Multiport Power Electronic Transformer with Shared Medium-Frequency Transformer. *IEEE Trans. Circuits Syst. II Express Briefs* **2021**, *68*, 727–731. [CrossRef]
66. Xiang, X.; Zhang, X.; Luth, T.; Merlin, M.M.C.; Green, T.C. A Compact Modular Multilevel DC–DC Converter for High Step-Ratio MV and HV Use. *IEEE Trans. Ind. Electron.* **2018**, *65*, 7060–7071. [CrossRef]
67. Gowaid, I.A.; Adam, G.P.; Massoud, A.M.; Ahmed, S.; Holliday, D.; Williams, B.W. Quasi Two-Level Operation of Modular Multilevel Converter for Use in a High-Power DC Transformer with DC Fault Isolation Capability. *IEEE Trans. Power Electron.* **2015**, *30*, 108–123. [CrossRef]
68. Mo, R.; Li, R.; Li, H. Isolated modular multilevel (IMM) DC/DC converter with energy storage and active filter function for shipboard MVDC system applications. In Proceedings of the 2015 IEEE Electric Ship Technologies Symposium (ESTS), Old Town Alexandria, VA, USA, 21–24 June 2015; pp. 113–117. [CrossRef]
69. Lu, Z.; Lin, L.; Wang, X.; Xu, C. LLC-MMC Resonant DC-DC Converter: Modulation Method and Capacitor Voltage Balance Control Strategy. In Proceedings of the 2020 IEEE Applied Power Electronics Conference and Exposition (APEC), New Orleans, LA, USA, 15–19 March 2020; pp. 2056–2061. [CrossRef]
70. Zhou, Q.; He, Z.; Li, Z.; Guan, R.; Zhou, B.; Huang, X.; Wang, L.; Xu, Q.; Chen, Y. A Step-Down Resonant Modular Multilevel DC/DC Converter with Extendable ZVS Range Based on Asymmetric Triangular Current. *IEEE Trans. Ind. Electron.* **2022**, *69*, 11088–11099. [CrossRef]
71. Essakiappan, S.; Krishnamoorthy, H.S.; Enjeti, P.; Balog, R.S.; Ahmed, S. Multilevel Medium-Frequency Link Inverter for Utility Scale Photovoltaic Integration. *IEEE Trans. Power Electron.* **2015**, *30*, 3674–3684. [CrossRef]
72. Luo, J.; Lin, K.; Li, J.; Xue, Y.; Zhang, X.-P. Cost Analysis and Comparison between Modular Multilevel Converter (MMC) and Modular Multilevel Matrix Converter (M3C) for Offshore Wind Power Transmission. In Proceedings of the 15th IET International Conference on AC and DC Power Transmission (ACDC 2019), Coventry, UK, 5–7 February 2019; pp. 1–6. [CrossRef]
73. Liu, S.; Wang, X.; Meng, Y.; Sun, P.; Luo, H.; Wang, B. A Decoupled Control Strategy of Modular Multilevel Matrix Converter for Fractional Frequency Transmission System. *IEEE Trans. Power Deliv.* **2017**, *32*, 2111–2121. [CrossRef]
74. Droguett, G.; Rojas, F.; Arancibia, D.; Diaz, M.; Mirzaeva, G.; Uriarte, M. Nearest Level Control for a three-phase to single-phase Modular Multilevel Converter for Solid State Transformers. In Proceedings of the 2018 IEEE International Conference on Automation/XXIII Congress of the Chilean Association of Automatic Control (ICA-ACCA), Concepcion, Chile, 17–19 October 2018; pp. 1–6. [CrossRef]
75. Ma, D.; Chen, W.; Shu, L.; Qu, X.; Zhan, X.; Liu, Z. A Multiport Power Electronic Transformer Based on Modular Multilevel Converter and Mixed-Frequency Modulation. *IEEE Trans. Circuits Syst. II Express Briefs* **2019**, *67*, 1284–1288. [CrossRef]
76. Far, A.A.J. *High Power DC/DC Converter and DC Hub Design Based on Modular Multilevel Topology*; Technical Report TR-SSEN-HVDC-UoA-001; The National HVDC Centre: Cumbernauld, UK, 2015.
77. Azimi, M.; Asadi, M. Optimum number of cascade cells for multilevel inverter considering redundancy strategies based on cost and reliability optimization. *IET Gener. Transm. Distrib.* **2023**, *17*, 4423–4436. [CrossRef]
78. Farzamkia, S.; Iman-Eini, H.; Khoshkbar-Sadigh, A.; Khaleghi, M.; Noushak, M. Comparative and Quantitative analyze on Reliability of MMC-Based and CHB-Based Drive Systems Considering Various Redundancy Strategies. In Proceedings of the 2020 11th Power Electronics, Drive Systems, and Technologies Conference (PEDSTC), Tehran, Iran, 4–6 February 2020; pp. 1–6. [CrossRef]
79. Akbar, S.M.; Hasan, A.; Watson, A.; Wheeler, P.; Odhano, S. Finite Control Set Model Predictive Control of Isolated DC/DC Modular Multilevel Converter. In Proceedings of the IECON 2020 the 46th Annual Conference of the IEEE Industrial Electronics Society, Singapore, 18–21 October 2020; pp. 5282–5289. [CrossRef]
80. Hillers, A.; Biela, J. Optimal design of the modular multilevel converter for an energy storage system based on split batteries. In Proceedings of the 2013 15th European Conference on Power Electronics and Applications (EPE), Lille, France, 2–6 September 2013; pp. 1–11. [CrossRef]

81. Hui, L.; Xie, X.; McDonald, A.; Chai, Z.; Yang, T.; Wu, Y.; Yang, W. Cost and reliability optimization of modular multilevel converter with hybrid submodule for offshore DC wind turbine. *Int. J. Electr. Power Energy Syst.* **2020**, *120*, 105994. [CrossRef]
82. Costa, L.F.; Hoffmann, F.; Buticchi, G.; Liserre, M. Comparative analysis of MAB dc-dc converters configurations in modular smart transformer. In Proceedings of the 2017 IEEE 8th International Symposium on Power Electronics for Distributed Generation Systems (PEDG), Florianopolis, Brazil, 17–20 April 2017; pp. 1–8. [CrossRef]
83. Kasper, M.; Bortis, D.; Kolar, J.W. Scaling and balancing of multi-cell converters. In Proceedings of the 2014 International Power Electronics Conference (IPEC-Hiroshima 2014—ECCE ASIA), Hiroshima, Japan, 18–21 May 2014; pp. 2079–2086. [CrossRef]
84. Huber, J. Conceptualization and Multi-Objective Analysis of Multi-Cell Solid-State Transformers. Ph.D. Thesis, ETH Zurich, Zürich, Switzerland, 2016. [CrossRef]
85. Magne, P.; Liu, P.; Bilgin, B.; Emadi, A. Investigation of impact of number of phases in interleaved dc-dc boost converter. In Proceedings of the 2015 IEEE Transportation Electrification Conference and Expo (ITEC), Dearborn, MI, USA, 14–17 June 2015; pp. 1–6. [CrossRef]
86. Huber, J.E.; Kolar, J.W. Optimum Number of Cascaded Cells for High-Power Medium-Voltage AC–DC Converters. *IEEE J. Emerg. Sel. Top. Power Electron.* **2017**, *5*, 213–232. [CrossRef]
87. Iyer, V.M.; Sharma, S.; Bhattacharya, S. A Methodology to Select the Number of Cascaded Cells for a Medium Voltage Multilevel AC-DC Solid State Transformer. In Proceedings of the 2020 IEEE Transportation Electrification Conference & Expo (ITEC), Chicago, IL, USA, 23–26 June 2020; pp. 55–61. [CrossRef]
88. Li, Y.; Zhang, Y.; Cao, R.; Liu, X.; Lv, C.; Liu, J. Redundancy design of modular DC solid-state transformer based on reliability and efficiency evaluation. *CPSS Trans. Power Electron. Appl.* **2021**, *6*, 115–126. [CrossRef]
89. Matthias Joachim Kasper. Analysis and Multi-Objective Optimization of Multi-Cell DC/DC and AC/DC Converter Systems. Ph.D. Thesis, ETH ZURICH, Zürich, Switzerland, 2016.
90. Beiranvand, H.; Rokrok, E.; Liserre, M. *Vf* -constrained $\eta\rho$-pareto Optim. Medium Freq. Transform. ISOP-DAB Convert. *IET Power Electron.* **2020**, *13*, 1984–1994. [CrossRef]
91. Makoschitz, M. Multi-megawatt charging to foster the mobility transition. *E I Elektrotechnik Und Informationstechnik* **2022**, *139*, 734–736. [CrossRef]
92. López, A.; Oliveira, T.H.; Arias, M.; Miaja, P.F.; Villarejo, J.A.; Fernández, A. Modular Fault Tolerant DC/DC Transformer Enabled by Natural Power Sharing. *IEEE Open J. Power Electron.* **2024**, *5*, 902–919. [CrossRef]
93. Huber, J.E.; Rothmund, D.; Kolar, J.W. Comparative evaluation of isolated front end and isolated back end multi-cell SSTs. In Proceedings of the 2016 IEEE 8th International Power Electronics and Motion Control Conference (IPEMC-ECCE Asia), Hefei, China, 22–26 May 2016; pp. 3536–3545. [CrossRef]
94. Oi, K.; Higa, H.; Morita, K.; Sato, Y. *Voltage Balancing Control of Bidirectional Input-Series Output—Series (ISOS) Dual Active Bridge DC/DC Converters without Auxiliary Circuits*; Technical Report Series No.192 2024 No.3; Meiden Review: Tokyo, Japan 2024.
95. Kroics, K.; Zakis, J.; Suzdalenko, A.; Gaigals, G. A simplified approach to input voltage balancing for series connected isolated DC-DC converters. In Proceedings of the 2016 18th European Conference on Power Electronics and Applications (EPE'16 ECCE Europe), Karlsruhe, Germany, 5–9 September 2016; pp. 1–10. [CrossRef]
96. Kim, M.; Park, H.P.; Jung, J.H. Hybrid Input Power Balancing Method of Modular Power Converters for High Efficiency, High Reliability, and Enhanced Dynamic Performance. *IEEE Trans. Ind. Electron.* **2022**, *69*, 5132–5141. [CrossRef]
97. Wang, P.; Chen, X.; Tong, C.; Zhang, X.; Jia, P.; Wen, C. High-frequency-link DC solid state transformer based on voltage self-balancing control for MVDC power distribution application. *IET Power Electron.* **2021**, *14*, 2620–2636. [CrossRef]
98. Sadat, A.R.; Krishnamoorthy, H.S. Fault-Tolerant ISOSP Solid-State Transformer for MVdc Distribution. *IEEE J. Emerg. Sel. Top. Power Electron.* **2021**, *9*, 6985–6996. [CrossRef]
99. Tian, J.; Mao, C.; Wang, D.; Nie, S.; Yang, Y. A Short-Time Transition and Cost Saving Redundancy Scheme for Medium-Voltage Three-Phase Cascaded H-Bridge Electronic Power Transformer. *IEEE Trans. Power Electron.* **2018**, *33*, 9242–9252. [CrossRef]
100. Alshawish, A.M.; Jafarishiadeh, S.; Ghasemi, A.; Shojaeighadikolaei, A.; Ahmadi, R. A New Fault Tolerant SST Topology and Operation Strategy for Alleviating HVAC Grid Faults. In Proceedings of the 2020 IEEE Kansas Power and Energy Conference (KPEC), Manhattan, KS, USA, 13–14 July 2020; pp. 1–6. [CrossRef]
101. Kasper, M.; Antivachis, M.; Bortis, D.; Kolar, J.W.; Deboy, G. 4D-Interleaving of Isolated ISOP Multi-Cell Converter Systems for Single Phase AC/DC Conversion. In Proceedings of the PCIM Europe 2016 International Exhibition and Conference for Power Electronics, Intelligent Motion, Renewable Energy and Energy Management, Nuremberg, Germany, 10–12 May 2016; pp. 1–9.
102. Vasiladiotis, M.; Rufer, A. A Modular Multiport Power Electronic Transformer with Integrated Split Battery Energy Storage for Versatile Ultrafast EV Charging Stations. *IEEE Trans. Ind. Electron.* **2015**, *62*, 3213–3222. [CrossRef]
103. Li, Z.; Hsieh, E.; Li, Q.; Lee, F.C. High-Frequency Transformer Design with Medium-Voltage Insulation for Resonant Converter in Solid-State Transformer. *IEEE Trans. Power Electron.* **2023**, *38*, 9917–9932. [CrossRef]
104. Liu, L.; Li, H.; Xue, Y.; Liu, W. Decoupled Active and Reactive Power Control for Large-Scale Grid-Connected Photovoltaic Systems Using Cascaded Modular Multilevel Converters. *IEEE Trans. Power Electron.* **2015**, *30*, 176–187. [CrossRef]

105. Follo, A.; Saborío-Romano, O.; Tedeschi, E.; Cutululis, N.A. Challenges in All-DC Offshore Wind Power Plants. *Energies* **2021**, *14*, 6057. [CrossRef]
106. Chuangpishit, S.; Tabesh, A.; Moradi-Sharbabk, Z.; Saeedifard, M. Topology Design for Collector Systems of Offshore Wind Farms with Pure DC Power Systems. *IEEE Trans. Ind. Electron.* **2014**, *61*, 320–328. [CrossRef]
107. Chen, W.W.; Zane, R.; Corradini, L. Isolated Bidirectional Grid-Tied Three-Phase AC–DC Power Conversion Using Series-Resonant Converter Modules and a Three-Phase Unfolder. *IEEE Trans. Power Electron.* **2017**, *32*, 9001–9012. [CrossRef]
108. Chen, W.; Riar, B.; Zane, R. Battery Integrated Modular Multifunction Converter for Grid Energy Storage. In Proceedings of the 2018 IEEE Energy Conversion Congress and Exposition (ECCE), Portland, OR, USA, 23–27 September 2018; pp. 2157–2163. [CrossRef]
109. Boris, J.S.; Evgny, H.N. Methods and Apparatus for Three-Phase Inverter with Reduced Energy Storage. US Patent US7839023B2, 22 January 2009.
110. Anderson, J.A.; Haider, M.; Bortis, D.; Kolar, J.W.; Kasper, M.; Deboy, G. New Synergetic Control of a 20 kW Isolated VIENNA Rectifier Front-End EV Battery Charger. In Proceedings of the 2019 20th Workshop on Control and Modeling for Power Electronics (COMPEL), Toronto, ON, Canada, 17–20 June 2019; pp. 1–8. [CrossRef]
111. Tahir, Y.; Khan, I.; Rahman, S.; Nadeem, M.F.; Iqbal, A.; Xu, Y.; Rafi, M. A state-of-the-art review on topologies and control techniques of solid-state transformers for electric vehicle extreme fast charging. *IET Power Electron.* **2021**, *14*, 1560–1576. [CrossRef]
112. Tu, H.; Feng, H.; Srdic, S.; Lukic, S. Extreme Fast Charging of Electric Vehicles: A Technology Overview. *IEEE Trans. Transp. Electrif.* **2019**, *5*, 861–878. [CrossRef]
113. Lee, M.; Yeh, C.S.; Yu, O.; Kim, J.W.; Choe, J.M.; Lai, J.S. Modeling and Control of Three-Level Boost Rectifier Based Medium-Voltage Solid-State Transformer for DC Fast Charger Application. *IEEE Trans. Transp. Electrif.* **2019**, *5*, 890–902. [CrossRef]
114. Koohi, P.; Watson, A.J.; Clare, J.C.; Soeiro, T.B.; Wheeler, P.W. A Survey on Multi-Active Bridge DC-DC Converters: Power Flow Decoupling Techniques, Applications, and Challenges. *Energies* **2023**, *16*, 5927. [CrossRef]
115. Zhang, Y.; Kotecha, R.; Mantooth, H.A.; Balda, J.C.; Zhao, Y.; Farnell, C. Cascaded bridgeless totem-pole multilevel converter with model predictive control for 400 V dc-powered data centers. In Proceedings of the 2017 IEEE Applied Power Electronics Conference and Exposition (APEC), Tampa, FL, USA, 26–30 March 2017; pp. 2745–2750. [CrossRef]
116. Lagier, T.; Ladoux, P.; Dworakowski, P. Potential of silicon carbide MOSFETs in the DC/DC converters for future HVDC offshore wind farms. *High Volt.* **2017**, *2*, 233–243. [CrossRef]
117. Fabre, J.; Ladoux, P.; Caron, H.; Verdicchio, A.; Blaquiere, J.M.; Flumian, D.; Sanchez, S. Characterization and Implementation of Resonant Isolated DC/DC Converters for Future MVdc Railway Electrification Systems. *IEEE Trans. Transp. Electrif.* **2021**, *7*, 854–869. [CrossRef]
118. Jammy, R.R.; Annamalai, K. A new configuration of seven-level quasi Z-source–based isolated inverter for renewable applications. *Int. Trans. Electr. Energy Syst.* **2019**, *29*, e2833. [CrossRef]
119. Pereira, T.; Hoffmann, F.; Zhu, R.; Liserre, M. A Comprehensive Assessment of Multiwinding Transformer-Based DC–DC Converters. *IEEE Trans. Power Electron.* **2021**, *36*, 10020–10036. [CrossRef]
120. Song, Y.; Madawala, U.K.; Thrimawithana, D.J.; Vilathgamuwa, M. Three-phase bi-directional wireless EV charging system with high tolerance to pad misalignment. *IET Power Electron.* **2019**, *12*, 2697–2705. [CrossRef]
121. Varghese, B.J.; Zane, R.A.; Kamineni, A.; Tavakoli, R.; Pantic, Z.; Chou, C.; Liu, L. Multi-Pad Receivers for High Power Dynamic Wireless Power Transfer. In Proceedings of the 2020 IEEE Energy Conversion Congress and Exposition (ECCE), Detroit, MI, USA, 11–15 October 2020; pp. 5162–5168. [CrossRef]
122. Ferreira Costa, L.; De Carne, G.; Buticchi, G.; Liserre, M. The Smart Transformer: A solid-state transformer tailored to provide ancillary services to the distribution grid. *IEEE Power Electron. Mag.* **2017**, *4*, 56–67. [CrossRef]
123. Liu, C.; Xu, X.; He, D.; Liu, H.; Tian, X.; Guo, Y.; Cai, G.; Ma, C.; Mu, G. Magnetic-Coupling Current-Balancing Cells based Input-parallel Output-parallel (IPOP) LLC Resonant Converter Modules for High-Frequency Isolation of DC Distribution Systems. *IEEE Trans. Power Electron.* **2015**, *31*, 6968–6979. [CrossRef]
124. Mo, R.; Yang, Y.; Chen, R.; Wu, W.; Hu, J.; Wen, H.; Wang, Y.; Fang, G.; Rodriguez, J. Low-Complexity Virtual-Vector-Based FCS-MPC with Unaffected Neutral-Point Voltage for Three-Phase T-Type Inverters. *IEEE J. Emerg. Sel. Top. Power Electron.* **2024**, *12*, 1683–1693. [CrossRef]
125. Busquets Monge, S.; Filba-Martinez, A.; Alepuz, S.; Calle-Prado, A. A Modulation Strategy to Operate Multilevel Multiphase Diode-Clamped and Active-Clamped DC–AC Converters at Low Frequency Modulation Indices with DC-Link Capacitor Voltage Balance. *IEEE Trans. Power Electron.* **2017**, *32*, 7521–7533. [CrossRef]
126. Jayakumar, V.; Chokkalingam, B.; Munda, J.L. A Comprehensive Review on Space Vector Modulation Techniques for Neutral Point Clamped Multi-Level Inverters. *IEEE Access* **2021**, *9*, 112104–112144. [CrossRef]
127. Yaramasu, V.; Wu, B.; Rivera, M.; Rodriguez, J. A New Power Conversion System for Megawatt PMSG Wind Turbines Using Four-Level Converters and a Simple Control Scheme Based on Two-Step Model Predictive Strategy—Part I: Modeling and Theoretical Analysis. *IEEE J. Emerg. Sel. Top. Power Electron.* **2014**, *2*, 3–13. [CrossRef]

128. Shao, S.; Clare, J.C.; Watson, A.J.; Wheeler, P.W. Detection and isolation of multiple faults in a modular multilevel converter based on a sliding mode observer. In Proceedings of the 2014 IEEE Energy Conversion Congress and Exposition (ECCE), Pittsburgh, PA, USA, 14–18 September 2014; pp. 3491–3495. [CrossRef]
129. Baolong Liu.; Zha, Y.; Zhang, T.; Chen, S. Sliding mode control for rectifier stage of solid state transformer. In Proceedings of the 2016 14th International Workshop on Variable Structure Systems (VSS), Nanjing, China, 1–4 June 2016; pp. 286–289. [CrossRef]
130. Bergna Diaz, G.; Formentini, A.; Zanchetta, P.; Tedeschi, E. Particle Swarm Optimization Tuning of Modular Multilevel Converters in a Time-Invariant Framework. In Proceedings of the 2019 IEEE 13th International Conference on Power Electronics and Drive Systems (PEDS), Toulouse, France, 9–12 July 2019; pp. 1–8. [CrossRef]
131. Tasiu, I.A.; Wang, H.; Liu, Z.; Zhang, Y.; Zhang, Q.; Meng, X.; Zhao, W. Robust fuzzy stabilization control for the traction converters in high-speed train. *Control Eng. Pract.* **2023**, *132*, 105423. [CrossRef]
132. Liu, X.; Qiu, L.; Fang, Y.; Wang, K.; Li, Y.; Rodríguez, J. A Fuzzy Approximation for FCS-MPC in Power Converters. *IEEE Trans. Power Electron.* **2022**, *37*, 9153–9163. [CrossRef]
133. Long, B.; He, Z.; Garcia, C.; Rodríguez, J.; Chong, K.T. A Model-Data Hybrid Driven Diagnosis Method for Open-Switch Faults in Three-Phase T-Type Grid-Connected Converters. *IEEE J. Emerg. Sel. Top. Power Electron.* **2024**, *12*, 3925–3935. [CrossRef]
134. Meng, X.; Hu, G.; Liu, Z.; Wang, H.; Zhang, G.; Lin, H.; Sadabadi, M.S. Neural Network-Based Impedance Identification and Stability Analysis for Double-Sided Feeding Railway Systems. *IEEE Trans. Transp. Electrif.* 2024, *Early Access*. [CrossRef]
135. Oliveira, T.; Mendes, A.; Caseiro, L. Model Predictive Control for Solid State Transformers: Advances and Trends. *Energies* **2022**, *15* , 8349. [CrossRef]
136. Garcia, C.; Mora, A.; Norambuena, M.; Rodriguez, J.; Aly, M.; Carnielutti, F.; Pereda, J.; Acuna, P.; Aguilera, R.; Tarisciotti, L. Model Predictive Control in Multilevel Inverters Part I: Basic Strategy and Performance Improvement. *IEEE Open J. Ind. Appl.* **2024**, *5*, 428–441. [CrossRef]
137. Norambuena, M.; Mora, A.; Garcia, C.; Rodriguez, J.; Aly, M.; Carnielutti, F.; Pereda, J.; Castillo, C.; Zhang, Z.; Yaramasu, V.; et al. Model Predictive Control in Multilevel Inverters Part II: Renewable Energies and Grid Applications. *IEEE Open J. Ind. Appl.* **2024**, *5*, 414–427. [CrossRef]
138. Liu, Y. Sector-based finite-set model predictive control of three-level grid-connected inverters. *UPB Sci. Bull. Ser. C* **2024**, *86*, 269–288.
139. Zhang, D.; Guacci, M.; Kolar, J.W.; Everts, J. Synergetic Control of a 3-ϕ Buck-Boost Current DC-Link EV Charger Considering Wide Output Range and Irregular Mains Conditions. In Proceedings of the 2020 IEEE 9th International Power Electronics and Motion Control Conference (IPEMC2020-ECCE Asia), Nanjing, China, 29 November–2 December 2020; pp. 1688–1695. [CrossRef]
140. Pou, J.; Pindado, R.; Boroyevich, D. Voltage-balance limits in four-level diode-clamped converters with passive front ends. *IEEE Trans. Ind. Electron.* **2005**, *52*, 190–196. [CrossRef]
141. Guan, Y.; Li, L. DC-link capacitor voltage balancing in five-level neutral point clamped Inverters using space vector modulation. In Proceedings of the IECON 2017—43rd Annual Conference of the IEEE Industrial Electronics Society, Beijing, China, 29 October–1 November 2017; pp. 1037–1042. [CrossRef]
142. Wang, K.; Zheng, Z.; Xu, L.; Li, Y. Neutral-Point Voltage Balancing Method for Five-Level NPC Inverters Based on Carrier-Overlapped PWM. *IEEE Trans. Power Electron.* **2021**, *36*, 1428–1440. [CrossRef]
143. Dai, L.; Wen, H.; Xu, P.; Feng, Z.; Wang, G.; Wang, X.; Rodriguez, J. Boundary Control Based Capacitor Voltage Balancing for Two/Three-Level Neutral-Point-Clamped Dual-Active-Bridge Converters. In Proceedings of the 10th International Power Electronics and Motion Control Conference (IPEMC2024-ECCE Asia), Chengdu, China, 17–20 May 2024; pp. 3101–3106. [CrossRef]
144. Pan, D.; Chen, M.; Wang, X.; Wang, H.; Blaabjerg, F.; Wang, W. EMI Modeling of Three-Level Active Neutral-Point-Clamped SiC Inverter Under Different Modulation Schemes. In Proceedings of the 2019 10th International Conference on Power Electronics and ECCE Asia (ICPE 2019—ECCE Asia), Busan, Republic of Korea, 27–30 May 2019; pp. 1–6. [CrossRef]
145. Sadigh, A.K.; Dargahi, V.; Corzine, K. Active voltage balancing of five-level H-bridge flying capacitor multicell converter controlled with level-shifted-carrier PWM. In Proceedings of the 2015 Clemson University Power Systems Conference (PSC), Clemson, SC, USA, 10–13 March 2015; pp. 1–8. [CrossRef]
146. Villanueva, E.; Correa, P.; Rodriguez, J.; Pacas, M. Control of a Single-Phase Cascaded H-Bridge Multilevel Inverter for Grid-Connected Photovoltaic Systems. *IEEE Trans. Ind. Electron.* **2009**, *56*, 4399–4406. [CrossRef]
147. Leon, J.I.; Vazquez, S.; Watson, A.J.; Franquelo, L.G.; Wheeler, P.W.; Carrasco, J.M. Feed-Forward Space Vector Modulation for Single-Phase Multilevel Cascaded Converters with Any DC Voltage Ratio. *IEEE Trans. Ind. Electron.* **2009**, *56*, 315–325. [CrossRef]
148. Le Goff, G.; Chorfi, I.; Alonso, C. Comparison of modular multilevel and flying capacitor converters made of wide bandgap switches for new MVDC grids. In Proceedings of the ELECTRIMACS 2024—The International Conference on Modeling and Simulation of Electric Machines, Converters and Systems, Castello de la Plana, Spain, 27–30 May 2024.
149. Ronanki, D.; Williamson, S.S. Modified Phase-disposition PWM Technique for Modular Multilevel Converters. In Proceedings of the 2018 IEEE Transportation Electrification Conference and Expo (ITEC), Long Beach, CA, USA, 13–15 June 2018; pp. 26–31. [CrossRef]

150. Wang, C.; Zheng, Z.; Wang, K.; Yang, B.; Zhou, P.; Li, Y. Analysis and Control of Modular Multilevel Matrix Converters Under Branch Fault Conditions. *IEEE Trans. Power Electron.* **2022**, *37*, 1682–1699. [CrossRef]
151. Kopacz, R.; Menzi, D.; Krismer, F.; Rąbkowski, J.; Kolar, J.W.; Huber, J. New single-stage bidirectional three-phase ac-dc solid-state transformer. *Electron. Lett.* **2024**, *60*, e13084. [CrossRef]
152. Czyz, P.; Papamanolis, P.; Guillod, T.; Krismer, F.; Kolar, J.W. New 40 kV/300 kVA Quasi-2-Level Operated 5-Level Flying Capacitor SiC "Super-Switch" IPM. In Proceedings of the 2019 10th International Conference on Power Electronics and ECCE Asia (ICPE 2019—ECCE Asia), Busan, Republic of Korea, 27–30 May 2019; pp. 813–820. [CrossRef]
153. Wang, L.; Zhang, D.; Wang, Y.; Wu, B.; Athab, H.S. Power and Voltage Balance Control of a novel Three-Phase Solid-State Transformer Using Multilevel Cascaded H-Bridge Inverters for Microgrid Applications. *IEEE Trans. Power Electron.* **2016**, *31*, 3289–3301. [CrossRef]
154. Zhang, X.; Zhou, L.; Qiu, D.; Xiao, W.; Zhang, B.; Xie, F. Phase-modular three-phase isolated bridgeless PFC converter. In Proceedings of the IECON 2015—41st Annual Conference of the IEEE Industrial Electronics Society, Yokohama, Japan, 9–12 November 2015; pp. 001723–001728. [CrossRef]
155. Isobe, T.; Barrera-Cardenas, R.A.; He, Z.; Zou, Y.; Terazono, K.; Tadano, H. Control of Three-Phase Solid-State Transformer with Phase-Separated Configuration for Minimized Energy Storage Capacitors. *IEEE J. Emerg. Sel. Top. Power Electron.* **2020**, *8*, 3014–3028. [CrossRef]
156. Ouyang, S.; Liu, J.; Chen, X.; Yang, Y. Control Strategy for Single-Phase Open-Circuit Operation of a Modular Solid-State Transformer. *IEEE Trans. Power Electron.* **2019**, *34*, 8555–8573. [CrossRef]
157. Yang, T.; Meere, R.; Feely, O.; O'Donnell, T. Performance of 3-phase 4-wire solid state transformer under imbalanced loads. In Proceedings of the 2014 IEEE PES T&D Conference and Exposition, Chicago, IL, USA, 14–17 April 2014; pp. 1–5. [CrossRef]
158. Chattopadhyay, R.; Viju Nair, R.; Bhattacharya, S. An Isolated DC-AC Converter Module Integrating Renewable Energy Source and Energy Storage for Cascaded Inverter. In Proceedings of the 2018 IEEE Energy Conversion Congress and Exposition (ECCE), Portland, OR, USA, 23–27 September 2018; pp. 3647–3652. [CrossRef]
159. Le, T.T.; Hakim, R.M.; Choi, S. A High-Efficiency Bidirectional Single-Stage AC-DC Converter Under Wide Voltage Range for Fast Chargers. *IEEE Trans. Power Electron.* **2023**, *38*, 4945–4956. [CrossRef]
160. Meng, F.; Man, Z.; Gao, L. A 12-pulse Rectifier Based on Power Electronic Phase-shifting Transformer. In Proceedings of the 2018 IEEE International Power Electronics and Application Conference and Exposition (PEAC), Shenzhen, China, 4–7 November 2018; pp. 1–4. [CrossRef]
161. Forouzesh, M.; Liu, Y.F.; Sen, P.C. Implementation of an Isolated Phase-Modular-Designed Three-Phase PFC Rectifier Based on Single-Stage LLC Converter. In Proceedings of the 2021 IEEE Energy Conversion Congress and Exposition (ECCE), Vancouver, BC, Canada, 10–14 October 2021; pp. 2266–2273. [CrossRef]
162. Saha, J.; Yadav, G.N.B.; Panda, S.K. A Matrix-Based Solid-State-Transformer For A Hybrid Nanogrid. In Proceedings of the 2018 IEEE International Conference on Power Electronics, Drives and Energy Systems (PEDES), Chennai, India, 18–21 December 2018; pp. 1–6. [CrossRef]
163. Schrittwieser, L.; Cortes, P.; Fassler, L.; Bortis, D.; Kolar, J.W. Modulation and Control of a Three-Phase Phase-Modular Isolated Matrix-Type PFC Rectifier. *IEEE Trans. Power Electron.* **2018**, *33*, 4703–4715. [CrossRef]
164. Chen, H.; Prasai, A.; Divan, D. Dyna-C: A Minimal Topology for Bidirectional Solid-State Transformers. *IEEE Trans. Power Electron.* **2017**, *32*, 995–1005. [CrossRef]
165. Hafez, B.; Krishnamoorthy, H.S.; Enjeti, P.; Ahmed, S.; Pitel, I.J. Medium voltage power distribution architecture with medium frequency isolation transformer for data centers. In Proceedings of the 2014 IEEE Applied Power Electronics Conference and Exposition—APEC 2014, Fort Worth, TX, USA, 16–20 March 2014; pp. 3485–3489. [CrossRef]
166. Krishnamoorthy, H.S.; Essakiappan, S.; Enjeti, P.N.; Balog, R.S.; Ahmed, S. A new multilevel converter for Megawatt scale solar photovoltaic utility integration. In Proceedings of the 2012 Twenty-Seventh Annual IEEE Applied Power Electronics Conference and Exposition (APEC), Orlando, FL, USA, 5–9 February 2012; pp. 1431–1438. [CrossRef]
167. Nair, A.C.; Fernandes, B.G. Solid-State Transformer Based Fast Charging Station for Various Categories of Electric Vehicles with Batteries of Vastly Different Ratings. *IEEE Trans. Ind. Electron.* **2021**, *68*, 10400–10411. [CrossRef]
168. Costa, L.F.; Buticchi, G.; Liserre, M. Modular Smart Transformer architectures: An overview and proposal of a interphase architecture. In Proceedings of the 2017 IEEE 8th International Symposium on Power Electronics for Distributed Generation Systems (PEDG), Florianopolis, Brazil, 17–20 April 2017; pp. 1–7. [CrossRef]
169. Ohno, T.; Mirić, S.; Guillod, T.; Krismer, F.; Huber, J.; Kolar, J.W. New Triple-Output Quad-Active-Bridge DC/DC Converter Employing a Four-Leg Inverter Input Stage. In Proceedings of the 2023 26th International Conference on Electrical Machines and Systems (ICEMS), Zhuhai, China, 5–8 November 2023; pp. 3984–3991. [CrossRef]
170. Pool-Mazun, E.I.; Sandoval, J.J.; Enjeti, P.N.; Pitel, I.J. An Integrated Solid-State Transformer with High-Frequency Isolation for EV Fast-Charging Applications. *IEEE J. Emerg. Sel. Top. Ind. Electron.* **2020**, *1*, 46–56. [CrossRef]

171. Vermulst, B.J.D.; Duarte, J.L.; Wijnands, C.G.E.; Lomonova, E.A. Quad-Active-Bridge Single-Stage Bidirectional Three-Phase AC–DC Converter with Isolation: Introduction and Optimized Modulation. *IEEE Trans. Power Electron.* **2017**, *32*, 2546–2557. [CrossRef]
172. Sal Y Rosas, D.; Chavez, D.; Frey, D.; Ferrieux, J.P. Single-Stage Isolated and Bidirectional Three-Phase Series-Resonant AC–DC Converter: Modulation for Active and Reactive Power Control. *Energies* **2022**, *15*, 8070. [CrossRef]
173. Keister, J.D.; Keister, T.L.; John, B.; Andreas, M.E. Power Management Utilizing Synchronous Common Coupling. US Patent US10811988B2, 20 October 2020.
174. Weise, N.; Mohapatra, K.; Mohan, N. Universal utility interface for Plug-in Hybrid electric vehicles with vehicle-to-grid functionality. In Proceedings of the Power and Energy Society General Meeting, Minneapolis, MN, USA, 25–29 July 2010; pp. 1–8. [CrossRef]
175. Younus, S.; Nardello, M.; Tosato, P.; Brunelli, D. Power Controlling, Monitoring and Routing Center Enabled by a DC-Transformer. *Energies* **2017**, *10*, 403. [CrossRef]
176. Bahmani, M.A.; Thiringer, T.; Rabiei, A.; Abdulahovic, T. Comparative Study of a Multi-MW High-Power Density DC Transformer with an Optimized High-Frequency Magnetics in All-DC Offshore Wind Farm. *IEEE Trans. Power Deliv.* **2016**, *31*, 857–866. [CrossRef]
177. Huber, J.E.; Kolar, J.W. Applicability of Solid-State Transformers in Today's and Future Distribution Grids. *IEEE Trans. Smart Grid* **2019**, *10*, 317–326. [CrossRef]
178. Hannan, M.A.; Ker, P.J.; Lipu, M.S.H.; Choi, Z.H.; Rahman, M.S.A.; Muttaqi, K.M.; Blaabjerg, F. State of the Art of Solid-State Transformers: Advanced Topologies, Implementation Issues, Recent Progress and Improvements. *IEEE Access* **2020**, *8*, 19113–19132. [CrossRef]
179. Jakka, V.N.S.R.; Shukla, A. A triple port active bridge converter based multi-fed power electronic transformer. In Proceedings of the 2016 IEEE Energy Conversion Congress and Exposition (ECCE), Milwaukee, WI, USA, 18–22 September 2016; pp. 1–8. [CrossRef]
180. Pham, V.L.; Wada, K. Applications of Triple Active Bridge Converter for Future Grid and Integrated Energy Systems. *Energies* **2020**, *13*, 1577. [CrossRef]
181. Frutos, P.; Briz, F.; Sanchez, A.; Guerrero, J.M. Quad-Active-Bridge as the basic cell of a MMC Based SST for DER and DESS Integration. In Proceedings of the 2019 IEEE 28th International Symposium on Industrial Electronics (ISIE), Vancouver, BC, Canada, 12–14 June 2019; pp. 2349–2355. [CrossRef]
182. Rashidi, M.; Baniahmed, S.; Nasiri, R.; Mazaheri, A.; Nasiri, A. Design and implementation of a multi winding high frequency transformer for MPSST application. In Proceedings of the IEEE 6th International Conference on Renewable Energy Research and Applications (ICRERA), 5–8 November 2017; pp. 491–494. [CrossRef]
183. Nie, J.; Yuan, L.; Wen, W.; Duan, R.; Shi, B.; Zhao, Z. Communication-Independent Power Balance Control for Solid State Transformer Interfaced Multiple Power Conversion Systems. *IEEE Trans. Power Electron.* **2020**, *35*, 4256–4271. [CrossRef]
184. Xu, J.; Mirić, S.; Bortis, D.; Blickenstorfer, M.; Hitz, M.; Kolar, J.W.; Huber, J. Automatic Time-Division Multiplexing for Inductive Power Transfer to Multiple Stainless-Steel-Enclosed Receivers. *IEEE J. Emerg. Sel. Top. Power Electron.* **2024**, *12*, 2333–2344. [CrossRef]
185. Rodrigues, W.A.; Oliveira, T.R.; Morais, L.M.F.; Rosa, A.H.R. Voltage and Power Balance Strategy without Communication for a Modular Solid State Transformer Based on Adaptive Droop Control. *Energies* **2018**, *11*, 1802. [CrossRef]
186. Zhu, C. *High-Efficiency, Medium-Voltage-Input, Solid-State-Transformer-Based 400-kW/1000 V/400 A Extreme Fast Charger for Electric Vehicles*; Technical Report EE–0008361, 1987553; DELTA: Livonia, MI, USA, 2023. [CrossRef]
187. Zhao, S.; Li, Q.; Lee, F.C.; Li, B. High-Frequency Transformer Design for Modular Power Conversion from Medium-Voltage AC to 400 VDC. *IEEE Trans. Power Electron.* **2018**, *33*, 7545–7557. [CrossRef]
188. Zheng, L.; Han, X.; Xu, C.; Kandula, R.; Graber, L.; Saeedifard, M.; Divan, D. 7.2 kV Three-Port SiC Single-Stage Current-Source Solid-State Transformer with 90 kV Lightning Protection. *IEEE Trans. Power Electron.* **2022**, *37*, 12080–12094. [CrossRef]
189. Mumuluh, R.N. Design Considerations for a High Power Medium Frequency Transformer for a DC-DC Converter Stage of a Solid State Transformer. Ph.D. Thesis, University College Dublin, School of Electrical and Electronic Engineering, Dublin, Ireland, 2016.
190. Siddique, H.A.B.; Ali, S.M.; De Doncker, R.W. DC collector grid configurations for large photovoltaic parks. In Proceedings of the 2013 15th European Conference on Power Electronics and Applications (EPE), Lille, France, 2–6 September 2013; pp. 1–10. [CrossRef]
191. Costa, L.F.; Buticchi, G.; Liserre, M. Comparison of basic power cells for quad-active-bridge DC-DC converter in smart transformer. In Proceedings of the 2015 17th European Conference on Power Electronics and Applications (EPE'15 ECCE-Europe), Geneva, Switzerland, 8–10 September 2015; pp. 1–10. [CrossRef]
192. Falcones, S.; Ayyanar, R.; Mao, X. A DC–DC Multiport-Converter-Based Solid-State Transformer Integrating Distributed Generation and Storage. *IEEE Trans. Power Electron.* **2013**, *28*, 2192–2203. [CrossRef]

193. Bandyopadhyay, S.; Purgat, P.; Qin, Z.; Bauer, P. A Multiactive Bridge Converter with Inherently Decoupled Power Flows. *IEEE Trans. Power Electron.* **2021**, *36*, 2231–2245. [CrossRef]
194. Buticchi, G.; Costa, L.F.; Barater, D.; Liserre, M.; Amarillo, E.D. A Quadruple Active Bridge Converter for the Storage Integration on the More Electric Aircraft. *IEEE Trans. Power Electron.* **2018**, *33*, 8174–8186. [CrossRef]
195. Zhao, C.; Round, S.D.; Kolar, J.W. An Isolated Three-Port Bidirectional DC-DC Converter with Decoupled Power Flow Management. *IEEE Trans. Power Electron.* **2008**, *23*, 2443–2453. [CrossRef]
196. Tao, H.; Kotsopoulos, A.; Duarte, J.; Hendrix, M. A Soft-Switched Three-Port Bidirectional Converter for Fuel Cell and Supercapacitor Applications. In Proceedings of the 2005 IEEE 36th Power Electronics Specialists Conference, Dresden, Germany, 16 June 2005; pp. 2487–2493. [CrossRef]
197. Wang, L.; Wang, Z.; Li, H. Asymmetrical Duty Cycle Control and Decoupled Power Flow Design of a Three-port Bidirectional DC-DC Converter for Fuel Cell Vehicle Application. *IEEE Trans. Power Electron.* **2012**, *27*, 891–904. [CrossRef]
198. Chen, Y.; Wang, P.; Li, H.; Chen, M. Power Flow Control in Multi-Active-Bridge Converters: Theories and Applications. In Proceedings of the 2019 IEEE Applied Power Electronics Conference and Exposition (APEC), Anaheim, CA, USA, 17–21 March 2019; pp. 1500–1507. [CrossRef]
199. Biswas, I.; Kastha, D.; Bajpai, P. Small Signal Modeling and Decoupled Controller Design for a Triple Active Bridge Multiport DC–DC Converter. *IEEE Trans. Power Electron.* **2021**, *36*, 1856–1869. [CrossRef]
200. Rahman, M.A.; Islam, M.R.; Muttaqi, K.M.; Sutanto, D. Design of a Multiloop Control Structure for Load-Disturbance Attenuation and Power-Mismatch Mitigation in Isolated Multiport Power Converters. *IEEE Trans. Ind. Electron.* **2022**, *69*, 8984–8996. [CrossRef]
201. Pereira, T.; Wei, Y.; Pascal, Y.; Mantooth, H.A.; Liserre, M. Self-Tuning Multiport Resonant DC/DC Converter Based on Actively-Controlled Inductors for Hybrid Storage System Integration. *IEEE Trans. Power Electron.* **2023**, *38*, 4787–4804. [CrossRef]
202. Cai, Y.; Gu, C.; Li, J.; Yang, J.; Buticchi, G.; Zhang, H. Dynamic Performance Enhancement of a Triple Active Bridge with Power Decoupling-Based Configurable Model Predictive Control. *IEEE Trans. Transp. Electrif.* **2023**, *9*, 3338–3349. [CrossRef]
203. Karami, M.; Baranwal, R. Optimal Control of Triple Active Bridge Based on Deep Machine Learning Techniques. In Proceedings of the 2022 IEEE Energy Conversion Congress and Exposition (ECCE), Detroit, MI, USA, 9–13 October 2022; pp. 1–7. [CrossRef]
204. Buticchi, G.; Farjudian, A.; Oh, J.; Tarisciotti, L. An ANN-Assisted Control for the Power Decoupling of a Multiple Active Bridge DC-DC Converter. In Proceedings of the IECON 2022–48th Annual Conference of the IEEE Industrial Electronics Society, Brussels, Belgium, 17–20 October 2022; pp. 1–6. [CrossRef]
205. Jafari, M.; Malekjamshidi, Z.; Lei, G.; Wang, T.; Platt, G.; Zhu, J. Design and Implementation of an Amorphous High-Frequency Transformer Coupling Multiple Converters in a Smart Microgrid. *IEEE Trans. Ind. Electron.* **2017**, *64*, 1028–1037. [CrossRef]
206. Pham, V.L.; Wada, K. Normalization Design of Inductances in Triple Active Bridge Converter for Household Renewable Energy System. *IEEJ J. Ind. Appl.* **2020**, *9*, 227–234. [CrossRef]
207. Costa, L.F.; Buticchi, G.; Liserre, M. Quad-Active-Bridge DC–DC Converter as Cross-Link for Medium-Voltage Modular Inverters. *IEEE Trans. Ind. Appl.* **2017**, *53*, 1243–1253. [CrossRef]
208. Hoffmann, F.; Lafrenz, J.L.; Liserre, M.; Vazquez, N. Multiwinding based Semi-Dual Active Bridge Converter. In Proceedings of the 2020 IEEE Applied Power Electronics Conference and Exposition (APEC), New Orleans, LA, USA, 15–19 March 2020; pp. 2142–2149. [CrossRef]
209. Wang, P.; Zhang, S.; Xu, D.; Lu, X. A series-resonance-based three-port converter with unified autonomous control method in DC microgrids. In Proceedings of the 2018 IEEE Applied Power Electronics Conference and Exposition (APEC), San Antonio, TX, USA, 4–8 March 2018; pp. 3270–3274. [CrossRef]
210. Krishnaswami, H.; Mohan, N. Three-Port Series-Resonant DC–DC Converter to Interface Renewable Energy Sources with Bidirectional Load and Energy Storage Ports. *IEEE Trans. Power Electron.* **2009**, *24*, 2289–2297. [CrossRef]
211. Tran, Y.K.; Dujić, D.; Barrade, P. Multiport resonant DC-DC converter. In Proceedings of the IECON 2015—41st Annual Conference of the IEEE Industrial Electronics Society, Yokohama, Japan, 9–12 November 2015; pp. 003839–003844. [CrossRef]
212. Tomas Manez, K.; Zhang, Z.; Ouyang, Z. Multi-port isolated LLC resonant converter for distributed energy generation with energy storage. In Proceedings of the 2017 IEEE Energy Conversion Congress and Exposition (ECCE), Cincinnati, OH, USA, 1–5 October 2017; pp. 2219–2226. [CrossRef]
213. Zhang, X.; Liu, H. A Novel Multi-Resonant Isolated Three-port Converter Capable of Achieving Power Decoupling. *IEICE Electron. Express* **2024**, *21*, 1–17. [CrossRef]
214. Rai, R.; Tummuru, N.R. Circulating and Leakage Power Flow Elimination Technique between Source Ports in Triple Active Bridge Topology. In Proceedings of the 2020 IEEE International Conference on Power Electronics, Smart Grid and Renewable Energy (PESGRE2020), Cochin, India, 2–4 January 2020; pp. 1–6. [CrossRef]
215. Chen, D.; Zhang, S.; Bai, B.; Zhang, Z.; Yang, Z. Study of the decoupling magnetic integrated high-frequency transformer for DC/DC converter. *IET Power Electron.* **2024**, *17*, 92–106. [CrossRef]

216. Ouyang, Z.; Zhang, Z.; Andersen, M.A.E.; Thomsen, O.C. Four Quadrants Integrated Transformers for Dual-Input Isolated DC–DC Converters. *IEEE Trans. Power Electron.* **2012**, *27*, 2697–2702. [CrossRef]
217. Ouyang, Z.; Andersen, M.A.E.; Thomsen, O.C. Decoupled power solution for dual-input isolated dc-dc converters using four quadrants integrated transformers (FQIT). In Proceedings of the 7th International Power Electronics and Motion Control Conference, Harbin, China, 2–5 June 2012; Volume 1, pp. 698–704. [CrossRef]
218. Fei, C.; Gadelrab, R.; Li, Q.; Lee, F.C. High-Frequency Three-Phase Interleaved LLC Resonant Converter with GaN Devices and Integrated Planar Magnetics. *IEEE J. Emerg. Sel. Top. Power Electron.* **2019**, *7*, 653–663. [CrossRef]
219. Nabih, A.; Li, Q. Design of 98.8% Efficient 400-to-48-V *LLC* Converter with Optimized Matrix Transformer and Matrix Inductor. *IEEE Trans. Power Electron.* **2023**, *38*, 7207–7225. [CrossRef]
220. Nabih, A.; Gadelrab, R.; Prakash, P.R.; Li, Q.; Lee, F.C. High Power Density 1 MHz 3 kW 400 V-48 V LLC Converter for Datacenters with improved Core Loss and Termination Loss. In Proceedings of the 2021 IEEE Applied Power Electronics Conference and Exposition (APEC), Phoenix, AZ, USA, 14–17 June 2021; pp. 304–309. [CrossRef]
221. Kougioulis, I.; Pal, A.; Wheeler, P.; Ahmed, M.R. An Isolated Multiport DC–DC Converter for Integrated Electric Vehicle On-Board Charger. *IEEE J. Emerg. Sel. Top. Power Electron.* **2023**, *11*, 4178–4198. [CrossRef]
222. Tarraf, R.; Morel, B.; Frey, D.; Leirens, S.; Carcouet, S.; Maynard, X.; Lembeye, Y. Modeling and Control of a Decoupled Hybrid-Fed Multi-Active Bridge (MAB) Converter. In Proceedings of the PCIM Europe 2023 International Exhibition and Conference for Power Electronics, Intelligent Motion, Renewable Energy and Energy Management, Nürnberg, Germany, 9–11 May 2023; pp. 1–9. [CrossRef]
223. Tarisciotti, L.; Zanchetta, P.; Watson, A.; Wheeler, P.; Clare, J.C.; Bifaretti, S. Multiobjective Modulated Model Predictive Control for a Multilevel Solid-State Transformer. *IEEE Trans. Ind. Appl.* **2015**, *51*, 4051–4060. [CrossRef]
224. Havrlík, M.; Libra, M.; Poulek, V.; Kouřím, P. Analysis of Output Signal Distortion of Galvanic Isolation Circuits for Monitoring the Mains Voltage Waveform. *Sensors* **2022**, *22*, 7769. [CrossRef] [PubMed]
225. Bojoi, I.; Armando, E.; Pellegrino, G.; Rosu, S. Self-commissioning of inverter nonlinear effects in AC drives. In Proceedings of the 2012 IEEE International Energy Conference and Exhibition (ENERGYCON), Florence, Italy, 9–12 September 2012; pp. 213–218. [CrossRef]
226. Yang, W.; Ma, J.; Zhu, M.; Hu, C.; Wen, S.; Liu, B. Fault Diagnosis and Tolerant Method of Open-circuit Fault for Triple Active-bridge DC-DC Converter. *Proc. CSEE* **2024**, *44*, 2374–2385. [CrossRef]
227. Wang, R.; Sun, Q.; Cheng, Q.; Ma, D. The Stability Analysis of a Multi-Port Single-Phase Solid-State Transformer in the Electromagnetic Timescale. *Energies* **2018**, *11*, 2250. [CrossRef]
228. Mishra, D.K.; Abbasi, M.H.; Eskandari, M.; Paudel, S.; Sahu, S.K.; Zhang, J.; Li, L. State–Space Modelling and Stability Analysis of Solid-State Transformers for Resilient Distribution Systems. *Appl. Sci.* **2024**, *14*, 1915. [CrossRef]
229. Granata, S.; Leuzzi, R.; Tresca, G.; Bassi, E.; Benzi, F.; Zanchetta, P. Stability Assessment Study for a Triple-Stage Three-Phase Solid-State Transformer. In Proceedings of the 2022 IEEE Energy Conversion Congress and Exposition (ECCE), Detroit, MI, USA, 9–13 October 2022; pp. 1–8. [CrossRef]
230. Khazraei, M.; Prabhala, V.A.K.; Ahmadi, R.; Ferdowsi, M. Solid-state transformer stability and control considerations. In Proceedings of the 2014 IEEE Applied Power Electronics Conference and Exposition—APEC 2014, Fort Worth, TX, USA, 16–20 March 2014; pp. 2237–2244. [CrossRef]
231. Rashidi, M.; Altin, N.N.; Ozdemir, S.S.; Bani-Ahmed, A.; Nasiri, A. Design and Development of a High-Frequency Multiport Solid-State Transformer with Decoupled Control Scheme. *IEEE Trans. Ind. Appl.* **2019**, *55*, 7515–7526. [CrossRef]
232. Mauger, M.J.; Chowdhury, V.R.; Kandula, P.; Divan, D. A Multiport DC Transformer to Enable Flexible Scalable DC as a Service. In Proceedings of the 2021 IEEE Energy Conversion Congress and Exposition (ECCE), Vancouver, BC, Canada, 10–14 October 2021; pp. 1197–1204. [CrossRef]

Disclaimer/Publisher's Note: The statements, opinions and data contained in all publications are solely those of the individual author(s) and contributor(s) and not of MDPI and/or the editor(s). MDPI and/or the editor(s) disclaim responsibility for any injury to people or property resulting from any ideas, methods, instructions or products referred to in the content.